

Article

# Robust Control Based on Adaptive Fuzzy Control of Double-Star Permanent Synchronous Motor Supplied by PWM Inverters for Electric Propulsion of Ships

Djamel Ziane <sup>1</sup>, Samir Zeglache <sup>2</sup>, Mohamed Fouad Benkhoris <sup>1,\*</sup> and Ali Djerioui <sup>2</sup><sup>1</sup> IREENA Laboratory, Nantes University, 44600 Saint Nazaire, France; djamel.ziane@univ-nantes.fr<sup>2</sup> Laboratoire d'Analyse des Signaux et Systèmes, Département of Electrical Engineering, Faculty of Technology, University of M'sila, BP 166 Ichbilia, M'sila 28000, Algeria; samir.zeglache@univ-msila.dz (S.Z.); ali.djerioui@univ-msila.dz (A.D.)

\* Correspondence: mohamed-fouad.benkhoris@univ-nantes.fr

**Abstract:** This study presents the development of an adaptive fuzzy control strategy for double-star PMSM-PWM inverters used in ship electrical propulsion. The approach addresses the current and speed tracking challenges of double-star permanent magnet synchronous motors (DSPMSMs) in the presence of parametric uncertainties. Initially, a modeling technique employing a matrix transformation method is introduced, generating decoupled and independent star windings to eliminate inductive couplings, while maintaining model consistency and torque control. The precise DSPMSM model serves as the foundation for an unknown nonlinear backstepping controller, approximated directly using an adaptive fuzzy controller. Through the Lyapunov direct method, system stability is demonstrated. All signals in the closed-loop system are ensured to be uniformly ultimately bounded (UUB). The proposed control system aims for low tracking errors, while also mitigating the impact of parametric uncertainties. The effectiveness of the adaptive fuzzy nonlinear control system is validated through tests conducted in hardware-in-the-loop (HIL) simulations, utilizing the OPAL-RT platform, OP4510.



**Citation:** Ziane, D.; Zeglache, S.; Benkhoris, M.F.; Djerioui, A. Robust Control Based on Adaptive Fuzzy Control of Double-Star Permanent Synchronous Motor Supplied by PWM Inverters for Electric Propulsion of Ships. *Mathematics* **2024**, *12*, 1451. <https://doi.org/10.3390/math12101451>

Academic Editors: Adrian Olaru, Gabriel Frumusanu and Catalin Alexandru

Received: 2 April 2024

Revised: 3 May 2024

Accepted: 4 May 2024

Published: 8 May 2024



**Copyright:** © 2024 by the authors. Licensee MDPI, Basel, Switzerland. This article is an open access article distributed under the terms and conditions of the Creative Commons Attribution (CC BY) license (<https://creativecommons.org/licenses/by/4.0/>).

**Keywords:** adaptive fuzzy control; double-star permanent magnet synchronous motor (DSPMSM); OPAL-RT (OP4510); model transformation

**MSC:** 93C42

## 1. Introduction

In the current context of energy transition and the search for sustainable solutions for maritime transport, the use of electric propulsion systems is emerging as a promising alternative. Double-star permanent magnet synchronous motors (DSPMSMs) supplied with pulse width modulation (PWM) inverters constitute a popular configuration for the electric propulsion of ships due to their high performance and increased energy efficiency [1]. In these large-scale drives, multi-phase machines offer crucial advantages [2], such as power distribution over multiple branches, a reduction in torque ripple amplitude, a decrease in current harmonics, and fault tolerance due to the high number of phases.

However, in marine environments, electric propulsion systems face significant variations in essential internal machine parameters, such as resistance, inductance, inertia, and friction. These internal variations, induced by dynamic operational conditions such as changes in load and speed, can substantially influence the performance of the propulsion system, thereby affecting power distribution and dynamic response. These internal variations are complemented by external variations, such as changing weather conditions and interactions with water. These external factors introduce disturbances, thus affecting the performance of the propulsion system and requiring dynamic adaptation of control strategies.

The DSPMSM has been the subject of several scientific articles, both in terms of modeling and control. The initial work emerged in the 1990s and 2000s, with proposed modeling and control approaches powered by voltage inverters applied for railway and ship propulsion [3,4].

Modeling work on the machine is diverse and conducted with various approaches. The difference lies in considering the machine as a six-phase machine with a connected neutral or considering it as equivalent to two three-phase machines with the two neutrals of the two machines separated. In the consideration as two three-phase motors, the modeling approach relies on the use of coordinate transformation based on synchronous rotating coordinate transformation (dq) [5,6].

Another modeling method exists which involves vector space decomposition (VSD), which is a machine modeling technique. The machine is divided into orthogonal subspaces using this method: one subspace producing a single flux/torque ( $\alpha$ - $\beta$ ) and numerous subspaces not producing flux/torque (x-y) [7].

The two methods mentioned earlier have been used as modeling tools in several works, including the double-star machine. In this article, we employ another approach to establish the model based on the general approach dynamical modeling of multi/three-phase machines developed in [8]. The elaborate modeling approach utilizes a novel decoupling transformation to eliminate couplings of multi-phase permanent magnet synchronous machines in a generic modular configuration.

In the literature, various approaches to synchronous machine control can be found, with most of them focusing on field-oriented control, classic direct torque control (DTC), adaptive fuzzy DTC, and neural DTC. If we analyze the different objectives targeted in these papers, we can summarize them into two components: optimal torque control and speed control. However, in these studies, the system under investigation is always considered to be time-invariant and without disturbance elements, thus not reflecting the reality of the system in real cases. This is because energy conversion systems undergo parametric variations related to heating, aging, magnetic circuit saturation, and other external constraints.

In Reference [9], a new method for direct torque control of permanent magnet synchronous machines (PMSMs) was presented. The simulation results confirmed the advantages of this approach compared to the conventional Direct Torque Control (DTC) approach. The proposed method offers a constant inverter switching frequency, reduces torque ripples, and exhibits good robustness to variations in stator resistance. However, it is observed that the only parametric variations considered are those related to stator resistance.

Vector control of rotating machines is recognized for its efficiency due to its simplicity of design and implementation, as well as its natural decoupling between flux and currents. This type of control is typically achieved using proportional–integral (PI) controllers, whose parameters are calculated directly from the machine characteristics using conventional analytical methods. However, this approach requires careful calculation and a good understanding of all machine parameters.

Historically, Fuzzy Logic Systems (FLSs) have a stellar reputation as effective approximators [10]. Their universal approximation qualities have led to their considerable usage in modeling and regulating unpredictable nonlinear systems. For diverse types of nonlinear systems, many adaptive fuzzy control methods have emerged in recent years [11–20]. The adaptive fuzzy control techniques for uncertain nonlinear systems were developed in [21–23], using a backstepping methodology. The stability of the closed-loop systems was achieved using the famous Lyapunov direct method. In this work, we suggest using this robust approximation method to address uncertainties and unknown dynamics inside the DSPMSM.

Motivated by the previous discussion, in this paper, the problem of currents and speed control is investigated for DSPMSM subject to parametric uncertainties via fuzzy approximation-based adaptive control. The FLS is used with the assistance of adaptive estimators in order to approximate unknown nonlinear dynamics. Additionally, a robust

adaptive compensation is utilized in order to mitigate the impact of parametric uncertainties and to correct approximation errors.

Our objective is to replace the PI controllers with adaptive controllers based on fuzzy logic in order to achieve a more robust control. We take into account the specific constraints encountered by maritime propulsion systems. Our proposal involves using an adaptive fuzzy control technique as an effective solution to mitigate the effects of internal parametric variations, such as stator resistance, machine inductances, inertia of the machine-load system, or viscous friction due to aging. This paper's key contributions are as follows: (i) the suggestion of an adaptive fuzzy control algorithm for DSPMSM that is resilient against uncertainty and can dampen the external disturbances; (ii) by integrating FLS, there is no reliance on the mathematical model; and (iii) the global closed-loop system is demonstrated to exhibit UUB stability.

The present study focuses on creating an adaptive fuzzy control method for DSPMSM systems that are exposed to external disturbances and uncertainty. The system dynamics are presumed to be unknown, and the controller settings are adjusted in response to the emergence of uncertainty. Making use of the fact that the system dynamics will be transformed into a strict-feedback form, if we include the models of uncertainty, external disturbances may affect the system model. A new fuzzy adaptive control approach is combined with a nonlinear control method to address this class of nonlinear systems. There are two control terms in the suggested adaptive control law. An adaptive fuzzy control rule is used as the initial control term to adjust the parameters online in order to deal with the uncertain system dynamics. To address the issue of fuzzy approximation errors, uncertainties, and external disturbances, the second term serves as a robust control by using the tangent hyperbolic function. The Lyapunov technique is used to examine the stability of the closed-loop system and guarantee the tracking error's convergence to zero.

The main contributions of this paper are the introduction of a new adaptive control strategy based on Takagi–Sugeno fuzzy inference systems. This strategy is designed to handle all types of uncertainties and external disturbances that may arise in the system dynamics. This work is compared to existing works in the same area, as referenced in [24–39]. The suggested research aims to address complex non-linear control issues with fewer assumptions compared to the existing literature. The following points encapsulate the contributions made by this work:

- The suggested fuzzy adaptive controller for uncertain systems reduces the amount of online learning parameters, making it easier to tune and suited for real-time implementations. Furthermore, regardless of the order of the nonlinear system, the suggested technique requires just basic fuzzy inference systems, while in [24–27], the number of updating parameters is still determined by the system's order.
- The control techniques proposed in [24–27] are based on backstepping, which is known to have the drawback of complexity growing. However, in the proposed method, the controllers have simpler structures and fewer design parameters, as the causes for the complexity growing problem were completely eliminated.
- The suggested adaptive control techniques may accomplish an a priori intended transient and steady-state performance in addition to ensuring the stability of the whole control system by adding prescribed performance. As a consequence, the suggested methods guarantee that the tracking error always converges to a predetermined, arbitrarily tiny residual set, which is not possible with the prior findings in the literature [24–26].
- By using the adaptive fuzzy control approach developed, the singularity and explosion of complexity concerns are effectively avoided in comparison to the backstepping control algorithms presented in [28,29]. In order to improve the tracking performance, the robust adaptive compensation techniques are also made to adjust for approximation errors and lessen the impact of parametric uncertainties.
- In contrast to the references mentioned in [30–34], the proposed controller is more flexible, as it does not require any knowledge of the mathematical model. On the other

hand, the suggested controller takes a systematic approach to handling unknown uncertainties and external disturbances.

- Restrictive assumptions regarding external perturbation were made by the authors in Refs. [35–37]. The external disturbance is modeled in Ref. [36] using time-varying free-models with derivable bounds, whereas in Ref. [35], it is described as an exogenous neutral stable system. In Ref. [37], it is divided into two parts, one of which represents an estimated portion and the other of which is generated by an exogenous system. The proposed work, on the other hand, assumes external perturbations under only the boundedness mild condition without considering any additional information.
- The developed controllers in Refs. [38–40] are intended for systems where the control gain must be a simple constant, which is a limiting constraint. The latter constraint is lifted in the suggested method to include a broader category of dynamical systems. To encompass a wide range of dynamical systems, such as inverted pendulums, induction motor drives, single-link robot arms, mass–spring–damper systems, flexible spacecraft, quadrotors, and many more, we actually presume that the system dynamics are unknown, with the control gain as an unknown nonlinear function.

Prior to presenting the obtained results, we delineate a modeling approach in the first section, followed by the mathematical development of the adaptive fuzzy control technique in the second section. Finally, the results of our tests, accompanied by a detailed analysis, are presented. These tests were conducted using the real-time simulator OP4510 from OPAL-RT.

## 2. Description of the Studied System

Our study focuses on a complex system, consisting of a permanent magnet synchronous machine with two stator windings. Each of these windings is powered by a three-phase inverter. To ensure the precise control of these two power electronic structures, we implemented adaptive fuzzy controllers, enabling the flexible and efficient management of the system in the presence of disturbances. The depicted system is illustrated in Figure 1.

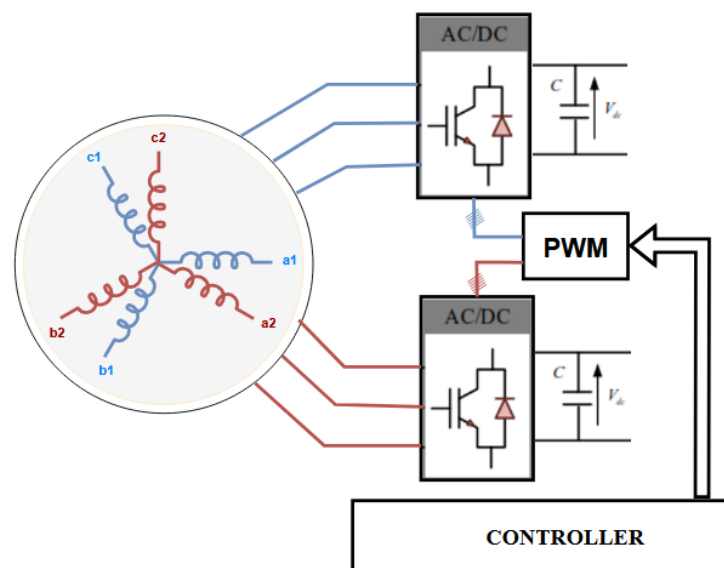


**Figure 1.** Structure of the considered system.

The PMSM is in the smoothed pole machine. The study is based on the following assumptions:

- The multi-phase winding consists of  $2 \times 3$  identical phases.
- Variable reluctance effects and saturation phenomena are neglected.
- Only the first space harmonic is taken into account.
- The temperature effects are neglected.

- (e) The capacitive effect between the windings is neglected.
- (f) The semiconductor components constituting the inverters are supposed to be perfect.

### 3. Mathematical Modeling of DSPMSM

As shown in Figure 2, the double-star permanent magnet synchronous motors (DSPMSM) considered in our study are composed of two three-phase windings phase-shifted by an angle,  $\gamma$ .

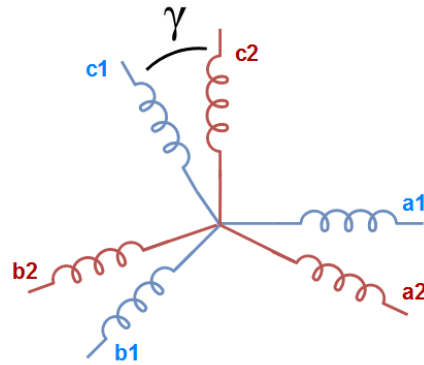


Figure 2. Double-star machine winding.

The establishment of the decoupled dynamic model of the DSPMSM is performed in three steps, which are described in the following subsections.

#### 3.1. Electrical Model in the (a1 b1 c1 a2 b2 c2) Frame

The general electrical equation of the DSPMSM in this natural basis can be written as follows:

$$[V_s] = R_s[I_s] + [L_s] \frac{d}{dt}[I_s] + [E_s] \tag{1}$$

where  $[V_s]$  represents the supply voltage vector of the stator windings. It is defined as follows:

$$[V_s] = \begin{bmatrix} [V_{s1}]^t & [V_{s2}]^t \end{bmatrix}^t \tag{2}$$

where

$$[V_{si}] = \begin{bmatrix} v_{ai} \\ v_{bi} \\ v_{ci} \end{bmatrix} \quad i = 1, 2 \tag{3}$$

where  $[I_s]$  represents the stator's currents vector. It is defined as follows:

$$[I_s] = \begin{bmatrix} [I_{s1}]^t & [I_{s2}]^t \end{bmatrix}^t \tag{4}$$

where

$$[I_{si}] = \begin{bmatrix} i_{ai} \\ i_{bi} \\ i_{ci} \end{bmatrix} \quad i = 1, 2 \tag{5}$$

where  $[E_s]$  represents the EMF voltage vector. It is defined as follows:

$$[E_s] = \begin{bmatrix} [E_{s1}]^t & [E_{s2}]^t \end{bmatrix}^t \tag{6}$$

where

$$[E_{si}] = \begin{bmatrix} E_{ai} \\ E_{bi} \\ E_{ci} \end{bmatrix} = -\sqrt{2}\omega\phi_f \begin{bmatrix} \sin(\theta - (i-1)\gamma) \\ \sin(\theta - \frac{2\pi}{3} - (i-1)\gamma) \\ \sin(\theta + \frac{2\pi}{3} - (i-1)\gamma) \end{bmatrix} \quad i = 1, 2 \tag{7}$$

where  $R_s$  is the resistance of each winding, and  $[L_s]$  is the stator's inductance matrix.  $[L_s]$  is defined as follows:

$$[L_s] = \begin{bmatrix} [L_{s1}] & [M_{s12}] \\ [M_{s12}]^t & [L_{s2}] \end{bmatrix} \tag{8}$$

where  $[L_{si}]$  ( $i = 1, 2$ ) represents the matrix inductance of each star and is defined as follows:

$$[L_{s1}] = [L_{s2}] = \begin{bmatrix} l_{fs} + M_{ss} & M_{ss} \cos(\frac{2\pi}{3}) & M_{ss} \cos(\frac{4\pi}{3}) \\ M_{ss} \cos(\frac{4\pi}{3}) & l_{fs} + M_{ss} & M_{ss} \cos(\frac{2\pi}{3}) \\ M_{ss} \cos(\frac{2\pi}{3}) & M_{ss} \cos(\frac{4\pi}{3}) & l_{fs} + M_{ss} \end{bmatrix} \tag{9}$$

where  $l_{fs}$  is the leakage inductance, and  $M_{ss}$  is the maximal mutual inductance between two windings.

$[M_{s12}]$  is the mutual inductance matrix between the two three windings. It is given by the following relation:

$$[M_{s12}] = \begin{bmatrix} M_{ss}(\gamma) & M_{ss}(\gamma + \frac{2\pi}{3}) & M_{ss}(\gamma + \frac{4\pi}{3}) \\ M_{ss}(\gamma + \frac{4\pi}{3}) & M_{ss}(\gamma) & M_{ss}(\gamma + \frac{2\pi}{3}) \\ M_{ss}(\gamma + \frac{2\pi}{3}) & M_{ss}(\gamma + \frac{4\pi}{3}) & M_{ss}(\gamma) \end{bmatrix} \tag{10}$$

From the inductance matrix, it can be easily shown that the matrix is fully coupled, so that the control the motor's currents in this frame are complicated.

### 3.2. Electrical Dynamical Model in the $(\alpha_1 \beta_1 \alpha_2 \beta_2)$

To write the electrical equations of the DSPSM in this reference frame, first we apply the Concordia transformation to each star (Figure 3A). Second, a rotation of an angle,  $\gamma$ , is applied to the second star (Figure 3B).

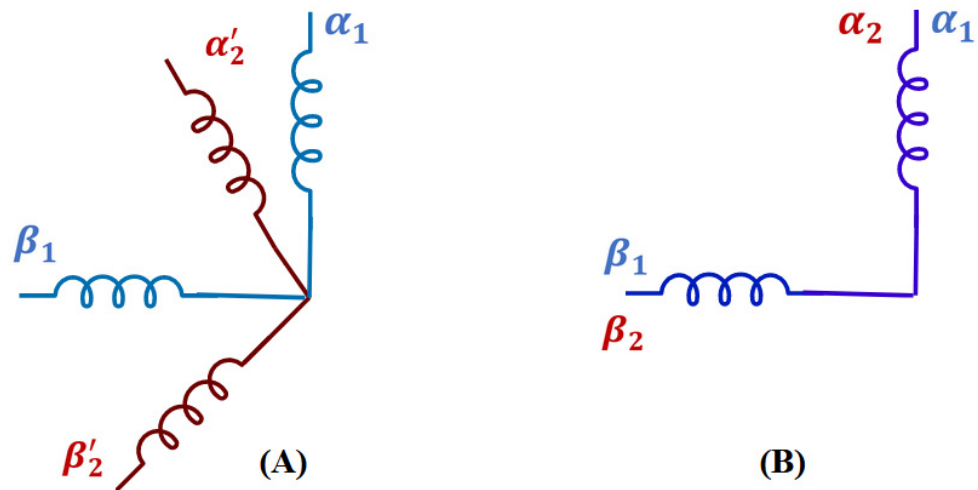


Figure 3. Equivalent windings in  $(\alpha_1 \beta_1 \alpha_2 \beta_2)$

This transformation from the reference frame  $(a_1 b_1 c_1 a_2 b_2 c_2)$  to the reference frame  $(\alpha_1 \beta_1 \alpha_2 \beta_2 o_2)$  is defined as follows:

$$[T_6]^t = \begin{bmatrix} \begin{bmatrix} [[T_{32}]]^t \\ [T_{31}]^t \end{bmatrix} & [0]_{3 \times 3} \\ [0]_{3 \times 3} & \begin{bmatrix} [[T_{32}] \cdot P(-\gamma)]^t \\ [T_{31}]^t \end{bmatrix} \end{bmatrix} \tag{11}$$

where

$$[T_{32}] = \sqrt{\frac{2}{3}} \begin{bmatrix} 1 & -\frac{1}{2} & -\frac{\sqrt{3}}{2} \\ 0 & -\frac{1}{2} & \frac{\sqrt{3}}{2} \end{bmatrix}^t \quad [T_{31}] = \begin{bmatrix} \frac{1}{\sqrt{2}} & \frac{1}{\sqrt{2}} & \frac{1}{\sqrt{2}} \end{bmatrix}^t \tag{12}$$

$$P(\gamma) = \begin{bmatrix} \cos(\gamma) & \sin(\gamma) \\ -\sin(\gamma) & \cos(\gamma) \end{bmatrix} \tag{13}$$

The electrical equation of the DSPMSM in this frame is as follows:

$$[T_6]^t [V_S] = R_S [T_6]^t [I_S] + [T_6]^t [L_S] \frac{d}{dt} [I_S] + [T_6]^t [E_S] \tag{14}$$

By applying this transformation, the stator’s inductance matrix  $[L_s]$ , the inductance matrix in this frame can be deduced:

$$[L_s'] = [T_6]^t [L_S] [T_6] \tag{15}$$

Thus, after the development of the calculation, we obtain the following:

$$[L_s'] = \begin{bmatrix} \begin{bmatrix} l_{fs} + \frac{3}{2}M_{ss} & 0 & 0 \\ 0 & l_{fs} + \frac{3}{2}M_{ss} & 0 \\ 0 & 0 & l_{fs} \end{bmatrix} & \begin{bmatrix} \frac{3}{2}M_{ss} & 0 & 0 \\ 0 & \frac{3}{2}M_{ss} & 0 \\ 0 & 0 & 0 \end{bmatrix} \\ \begin{bmatrix} \frac{3}{2}M_{ss} & 0 & 0 \\ 0 & \frac{3}{2}M_{ss} & 0 \\ 0 & 0 & 0 \end{bmatrix} & \begin{bmatrix} l_{fs} + \frac{3}{2}M_{ss} & 0 & 0 \\ 0 & l_{fs} + \frac{3}{2}M_{ss} & 0 \\ 0 & 0 & l_{fs} \end{bmatrix} \end{bmatrix} \tag{16}$$

The inductance matrix  $[L_s']$  is not completely diagonal. In this new reference frame, windings following the same axis,  $\alpha$  or  $\beta$ , are coupled. Therefore, their mutual inductance is non-zero and equal to  $3M_{ss}/2$ . However, since the axes  $\alpha$  and  $\beta$  are orthogonal, the mutual inductances between the windings following these axes are zero.

The electromagnetic torque in this frame is defined as follows:

$$\Gamma = \frac{e_{a1}i_{\alpha1} + e_{\beta1}i_{\beta1} + e_{a2}i_{\alpha2} + e_{\beta2}i_{\beta2}}{\Omega} \tag{17}$$

It is important to notice that the transformation  $P(\gamma)$  applied to the second star and defined above only introduces a rotation of the EMF vector and does not modify its module. We then have the following:

$$\begin{aligned} e_{\alpha1} &= e_{\alpha2} = e_{\alpha} = -\sqrt{3}\omega\varphi_f \sin(\theta) \\ e_{\beta1} &= e_{\beta2} = e_{\beta} = \sqrt{3}\omega\varphi_f \cos(\theta) \end{aligned} \tag{18}$$

Then, the torque expression can be simplified and becomes as follows:

$$\Gamma = \frac{e_a(i_{\alpha1} + i_{\alpha2}) + e_{\beta}(i_{\beta1} + i_{\beta2})}{\Omega} \tag{19}$$

### 3.3. Electrical Dynamical Model in the $(\alpha \beta z_1 z_2 z_3 z_4)$

Based in the next expression of the torque, a new change of variable based on the sum of the currents is introduced. And in order to preserve the order of the system (6), we introduce the difference in currents which will also have the advantage of eliminating the coupling terms present in the inductance matrix. These current differences have no effect on the torque, but this ensures the bijectivity of the transformation matrix from one frame of reference to another. Thus, in order to write the electrical equations in the new

frame, where the inductance matrix is diagonal, we also apply it to the voltage, current, and EMF vectors.

From this, to transform the quantities of the  $(\alpha_1 \beta_1 \alpha_2 \beta_2 \alpha_3 \beta_3)$  reference to this new reference, called  $(\alpha \beta z_1 z_2 z_3 z_4)$ , the following normalized matrix is defined:

$$\begin{bmatrix} x_\alpha \\ x_\beta \\ x_{z1} \\ x_{z2} \\ x_{z3} \\ x_{z'} \end{bmatrix} = \frac{1}{\sqrt{2}} \begin{bmatrix} \begin{bmatrix} 1 & 0 & 0 \\ 0 & 1 & 0 \\ 0 & 0 & 1 \end{bmatrix} & \begin{bmatrix} 1 & 0 & 0 \\ 0 & 1 & 0 \\ 0 & 0 & 1 \end{bmatrix} \\ \begin{bmatrix} 1 & 0 & 0 \\ 0 & 1 & 0 \\ 0 & 0 & 1 \end{bmatrix} & -\begin{bmatrix} 1 & 0 & 0 \\ 0 & 1 & 0 \\ 0 & 0 & 1 \end{bmatrix} \end{bmatrix} \begin{bmatrix} x_{\alpha1} \\ x_{\beta1} \\ x_{\alpha2} \\ x_{\alpha2} \\ x_{\beta1} \\ x_{\alpha2} \end{bmatrix} \tag{20}$$

where  $x = v, i,$  and  $e$ .

By applying this transformation to the electrical equation in  $(\alpha_1 \beta_1 \alpha_2 \beta_2 \alpha_3 \beta_3)$ , the new electrical equation is obtained.

Now, the electrical equation in this  $(\alpha\beta z_1 z_2 z_3 z_4)$  frame can be easily deduced:

$$\begin{cases} v_\alpha = R_s i_\alpha + L_c M_{ss} \frac{d}{dt}(i_\alpha) - \sqrt{6} \omega \varphi_f \sin(\theta) \\ v_\beta = R_s i_\beta + L_c \frac{d}{dt}(i_\beta) + \sqrt{6} \omega \varphi_f \cos(\theta) \\ v_{zj} = R_s i_{zj} + l_{fs} \frac{d}{dt}(i_{zj}) \quad j = 1, 4 \end{cases} \tag{21}$$

where

$$L_c = l_{fs} + 3M_{ss} \tag{22}$$

Finally, the transformation matrix from the initial the  $(a_1 b_1 c_1 a_2 b_2 c_2)$  coordinate system to the final  $(\alpha \beta z_1 z_2 z_3 z_4)$  coordinate system is as follows:

$$[T]^t = \frac{1}{\sqrt{2}} \begin{bmatrix} \begin{bmatrix} 1 & 0 & 0 \\ 0 & 1 & 0 \\ 0 & 0 & 1 \end{bmatrix} & \begin{bmatrix} 1 & 0 & 0 \\ 0 & 1 & 0 \\ 0 & 0 & 1 \end{bmatrix} \\ \begin{bmatrix} 1 & 0 & 0 \\ 0 & 1 & 0 \\ 0 & 0 & 1 \end{bmatrix} & -\begin{bmatrix} 1 & 0 & 0 \\ 0 & 1 & 0 \\ 0 & 0 & 1 \end{bmatrix} \end{bmatrix} \begin{bmatrix} \begin{bmatrix} [T_{32}]^t \\ [T_{31}]^t \end{bmatrix} & [0]_{3 \times 3} \\ [0]_{3 \times 3} & \begin{bmatrix} [[T_{32}] \cdot P(-\gamma)]^t \\ [T_{31}]^t \end{bmatrix} \end{bmatrix} \tag{23}$$

In the case where the angular offset is  $\gamma = \frac{\pi}{6}$ , this leads to the matrix T, as presented in Equation (24):

$$[T] = \begin{bmatrix} \sqrt{\frac{1}{3}} & -\sqrt{\frac{1}{11}} & -\sqrt{\frac{1}{11}} & \frac{1}{2} & -\frac{1}{2} & 0 \\ 0 & \frac{-1}{2} & \frac{1}{2} & -\sqrt{\frac{1}{11}} & -\sqrt{\frac{1}{11}} & \sqrt{\frac{1}{3}} \\ \sqrt{\frac{1}{6}} & \sqrt{\frac{1}{6}} & \sqrt{\frac{1}{6}} & \sqrt{\frac{1}{6}} & \sqrt{\frac{1}{6}} & \sqrt{\frac{1}{6}} \\ \sqrt{\frac{1}{3}} & -\sqrt{\frac{1}{11}} & -\sqrt{\frac{1}{11}} & -\frac{1}{2} & \frac{1}{2} & 0 \\ 0 & -\frac{1}{2} & \frac{1}{2} & \sqrt{\frac{1}{11}} & \sqrt{\frac{1}{11}} & \sqrt{\frac{1}{11}} \\ \sqrt{\frac{1}{6}} & \sqrt{\frac{1}{6}} & \sqrt{\frac{1}{6}} & -\sqrt{\frac{1}{6}} & -\sqrt{\frac{1}{6}} & -\sqrt{\frac{1}{6}} \end{bmatrix} \tag{24}$$

### 3.4. Electrical Equation in Park's Frame

By applying the classical Park transformation only to the ab component, the dynamical electrical model in the  $(dqzj)_{j=1,4}$  frame can be established:

$$\begin{cases} V_d = R i_d + L_c \frac{d}{dt} i_d - \omega L_c i_q \\ V_q = R i_q + L_c \frac{d}{dt} i_q + \omega L_c i_d + \sqrt{6} \omega \varphi_f \\ V_{zj} = R i_{zj} + l_{fs} \frac{d}{dt} i_{zj} \quad j = 1, 4 \end{cases} \tag{25}$$

The electromagnetic torque equation is as follows:

$$\Gamma = \frac{e_d i_d + e_q i_q}{\Omega} = \frac{e_q i_q}{\Omega} = p \frac{e_q i_q}{\omega} = \sqrt{6} p \varphi_f i_q \tag{26}$$

### 3.5. Mechanical Equation

The mechanical equation is classical, and it is given by the following relationship:

$$J \frac{d\Omega}{dt} = \Gamma - \Gamma_l - f_v \Omega \tag{27}$$

where  $J$  is the motor inertia,  $\Gamma_l$  is the load torque, and  $f_v$  is the viscous friction.

### 3.6. Modeling Approach for Control Strategies

By combining the electrical Equations (25) and (26) with the mechanical Equation (27), we obtain the model of the DSPMSM used to develop the control strategy, as depicted in Equation (28):

$$\begin{cases} \frac{d\Omega}{dt} = -\frac{\Gamma_l}{J} - \frac{f_v}{J} \Omega + \frac{\sqrt{6} p \varphi_f}{J} i_q \\ \frac{di_q}{dt} = -p\Omega i_d - \frac{\sqrt{6} \varphi_f}{L_c} p\Omega - \frac{R}{L_c} i_q + \frac{1}{L_c} V_q \\ \frac{di_d}{dt} = p\Omega i_q - \frac{R}{L_c} i_d + \frac{1}{L_c} V_d \\ \frac{di_{zj}}{dt} = \frac{R}{l_{fs}} i_{zj} + \frac{1}{l_{fs}} V_{zj} \quad \text{for } j = 1, \dots, 4 \end{cases} \tag{28}$$

The DSPMSM model in (28) may be reorganized in the following manner:

$$\begin{cases} \frac{d\Omega}{dt} = f_1 + g_1 i_q \\ \frac{di_q}{dt} = f_2 + g_2 V_q \\ \frac{di_d}{dt} = f_3 + g_3 V_d \\ \frac{di_{zj}}{dt} = f_4 i_{zj} + g_4 V_{zj} \quad \text{for } j = 1, \dots, 4 \end{cases} \tag{29}$$

where  $f_1, \dots, f_4$  and  $g_1, \dots, g_4$  are unknown continuous nonlinear functions.

$$\begin{cases} f_1 = -\frac{\Gamma_l}{J} - \frac{f_v}{J} \Omega, \quad \text{and} \quad g_1 = \frac{\sqrt{6} p \varphi_f}{J} \\ f_2 = -p\Omega i_d - \frac{\sqrt{6} \varphi_f}{L_c} p\Omega - \frac{R}{L_c} i_q, \quad g_2 = g_3 = \frac{1}{L_c} \\ f_3 = p\Omega i_q - \frac{R}{L_c} i_d \\ f_4 = \frac{R}{l_{fs}}, \quad g_4 = \frac{1}{l_{fs}} \end{cases} \tag{30}$$

## 4. Nonlinear Control Design-Based Model for DSPMSM

In this section, a nonlinear control design-based model for DSPMSM is synthesized in order to obtain good tracking performances for speed and torque; to achieve this goal, some realistic assumptions are introduced.

**Assumption 1.** The reference signals  $\Omega^*$ ,  $i_q^*$ ,  $i_d^*$ , and  $i_{zj}^*$ , as well as their first derivatives, exhibit boundedness and continuity.

**Assumption 2.** The rotor speed, and stator current are measurable greatness.

For the reference signals  $\Omega^*$ ,  $i_q^*$ ,  $i_d^*$ , and  $i_{zj}^*$ , we may define the tracking errors and their corresponding filtered errors as follows:

$$Z_\Omega = \Omega^* - \Omega; S_\Omega = Z_\Omega + \lambda_\Omega \int_0^t Z_\Omega(\tau) d\tau; \text{ with } Z_\Omega(0) = 0 \tag{31}$$

$$Z_{i_q} = i_q^* - i_q; S_{i_q} = Z_{i_q} + \lambda_{i_q} \int_0^t Z_{i_q}(\tau) d\tau; \text{ with } Z_{i_q}(0) = 0 \tag{32}$$

$$Z_{i_d} = i_d^* - i_d; S_{i_d} = Z_{i_d} + \lambda_{i_d} \int_0^t Z_{i_d}(\tau) d\tau; \text{ with } Z_{i_d}(0) = 0 \tag{33}$$

$$\dots Z_{i_{z_j}} = i_{z_j}^* - i_{z_j}; S_{z_j} = Z_{i_{z_j}} + \lambda_{z_j} \int_0^t Z_{z_j}(\tau) d\tau; \text{ with } Z_{z_j}(0) = 0 \text{ } j = 1, \dots, 4 \tag{34}$$

where  $\lambda_\Omega, \lambda_{i_q}, \lambda_{i_d}$  and  $\lambda_{z_j}$  are positive design parameters.

The control objectives are  $i_q^* = i_d = 0, i_q = i_q^*$  and  $i_{z_j} = i_{z_j}^* = 0$  for  $j = 1, \dots, 4$ .

**Step 1. Speed control.**

Using Equation (28), the first filtered error dynamic of (31) is provided by the following:

$$\dot{S}_\Omega = \dot{\Omega}^* - f_1 - g_1 i_q^* + \lambda_\Omega Z_\Omega \tag{35}$$

Let us select the Lyapunov function candidate as  $V_{1\Omega} = \frac{1}{2} S_\Omega^2$ , and its time derivative is as follows:

$$\dot{V}_{1\Omega} = S_\Omega \dot{S}_\Omega = S_\Omega \left( \dot{\Omega}^* - f_1 - g_1 i_q^* + \lambda_\Omega Z_\Omega \right) \tag{36}$$

The control law,  $i_q^*$ , is formulated as follows:

$$i_q^* = \frac{1}{g_1} \left[ \dot{\Omega}^* - f_1 + \lambda_\Omega Z_\Omega \right] + c_\Omega S_\Omega \tag{37}$$

where  $c_\Omega$  is the positive design parameter.

It is simply verifiable, using (9), that

$$\dot{V}_{1\Omega} = -c_\Omega S_\Omega^2 < 0 \tag{38}$$

**Step 2. Currents control.**

Select the candidate Lyapunov function with augmentation as follows:

$$\begin{cases} V_{2i} = \frac{1}{2} S_{i_q}^2 + \frac{1}{2} S_{i_d}^2 \\ V_{2j} = \frac{1}{2} S_{z_j}^2 \text{ for } j = 1, \dots, 4 \end{cases} \tag{39}$$

The filtered error dynamics of (4) to (6) are given by the following:

$$\dot{S}_{i_q} = \frac{di_q^*}{dt} - f_2 - g_2 V_q + \lambda_{i_q} Z_{i_q} \tag{40}$$

$$\dot{S}_{i_d} = \frac{di_d^*}{dt} - f_3 - g_3 V_d + \lambda_{i_d} Z_{i_d} \tag{41}$$

$$\dot{S}_{z_j} = \frac{di_{z_j}^*}{dt} - f_4 - g_4 V_{z_j} + \lambda_{z_j} Z_{z_j} \text{ for } j = 1, \dots, 4 \tag{42}$$

After that, the time derivative of (39) is written as follows:

$$\begin{cases} \dot{V}_{2i} = S_{i_q} \left( \frac{di_q^*}{dt} - f_2 - g_2 V_q + \lambda_{i_q} Z_{i_q} \right) + S_{i_d} \left( \frac{di_d^*}{dt} - f_3 - g_3 V_d + \lambda_{i_d} Z_{i_d} \right) \\ \dot{V}_{2j} = S_{z_j} \left( \frac{di_{z_j}^*}{dt} - f_4 - g_4 V_{z_j} + \lambda_{z_j} Z_{z_j} \right) \text{ for } j = 1, \dots, 4 \end{cases} \tag{43}$$

The control laws  $V_q, V_d$ , and  $V_{z_j}$  for  $j = 1, \dots, 4$  are designed as follows:

$$V_q = \frac{1}{g_2} \left[ \frac{di_q^*}{dt} - f_2 + \lambda_{i_q} Z_{i_q} \right] + c_{i_q} S_{i_q} \tag{44}$$

$$V_d = \frac{1}{g_3} \left[ \frac{di_d^*}{dt} - f_3 + \lambda_{id}Z_{id} \right] + c_{id}S_{id} \tag{45}$$

$$V_{zj} = \frac{1}{g_4} \left[ \frac{di_{zj}^*}{dt} - f_4 + \lambda_{zj}Z_{zj} \right] + c_{zj}S_{zj} \text{ for } j = 1, \dots, 4 \tag{46}$$

where  $c_{i_q}$ ,  $c_{i_d}$ , and  $c_{z_j}$  for  $j = 1, \dots, 4$  are positive design parameters.

Using (44), (45), and (46), it is simple to demonstrate that

$$\begin{cases} \dot{V}_{2i} = -c_{i_q}S_{i_q}^2 - c_{i_d}S_{i_d}^2 < 0 \\ \dot{V}_{zj} = -c_{zj}S_{zj}^2 < 0 \end{cases} \tag{47}$$

The control laws  $i_q^*$ ,  $V_q$ ,  $V_d$ , and  $V_{zj}$  for  $j = 1, \dots, 4$  can be expressed as follows [25]:

$$i_q^* = I_q^* + c_{\Omega}S_{\Omega} \tag{48}$$

$$V_q = U_q + c_{i_q}S_{i_q} \tag{49}$$

$$V_d = U_d + c_{i_d}S_{i_d} \tag{50}$$

$$V_{zj} = U_{zj} + c_{zj}S_{zj} \text{ for } j = 1, \dots, 4 \tag{51}$$

where the ideal controls  $I_q^*$ ,  $U_q$ ,  $U_d$ , and  $U_{zj}$  for  $j = 1, \dots, 4$  are given by the following:

$$I_q^* = \frac{1}{g_1} \left[ \dot{\Omega}^* - f_1 + \lambda_{\Omega}Z_{\Omega} \right] \tag{52}$$

$$U_q = \frac{1}{g_2} \left[ \frac{di_q^*}{dt} - f_2 + \lambda_{i_q}Z_{i_q} \right] \tag{53}$$

$$U_d = \frac{1}{g_3} \left[ \frac{di_d^*}{dt} - f_3 + \lambda_{i_d}Z_{i_d} \right] \tag{54}$$

$$U_{zj} = \frac{1}{g_4} \left[ \frac{di_{zj}^*}{dt} - f_4 + \lambda_{zj}Z_{zj} \right] \text{ for } j = 1, \dots, 4 \tag{55}$$

Given that  $\dot{V}_{1\Omega}(t)$ ,  $\dot{V}_{2i}(t)$ , and  $\dot{V}_{zj}(t)$  for  $j = 1, \dots, 4$  are negative semi-definite, it follows that  $V_{1\Omega}(t) \leq V_{1\Omega}(0)$ ,  $V_{2i}(t) \leq V_{2i}(0)$  and  $V_{zj}(t) \leq V_{zj}(0)$  for  $j = 1, \dots, 4$ .

Consequently,  $S_{\Omega}$ ,  $S_{i_q}$ ,  $S_{i_d}$ , and  $S_{z_j}$  for  $j = 1, \dots, 4$  exhibit uniform boundedness. This indicates that the closed-loop signals  $S_{\Omega}$ ,  $S_{i_q}$ ,  $S_{i_d}$ , and  $S_{z_j}$  for  $j = 1, \dots, 4$ ,  $i_q^*$ ,  $V_q$ ,  $V_d$ , and  $V_{zj}$  for  $j = 1, \dots, 4$  are constrained within certain limits.

Given that  $V_{1\Omega}(0)$ ,  $V_{2i}(0)$ , and  $V_{zj}(0)$  for  $j = 1, \dots, 4$  are limited, and  $V_{1\Omega}$ ,  $V_{2i}$ , and  $V_{zj}$  for  $j = 1, \dots, 4$  are non-increasing and limited from below, it can be concluded that the  $\lim_{t \rightarrow \infty} V_{1\Omega}(t)$ ,  $\lim_{t \rightarrow \infty} V_{2i}(t)$ , and  $\lim_{t \rightarrow \infty} V_{zj}(t)$  for  $j = 1, \dots, 4$  exist. By using Barbalat's Lemma [41], it can be deduced that  $(S_{\Omega}, S_{i_q}, S_{i_d}, S_{z_j} \text{ for } j = 1, \dots, 4) \rightarrow 0$  as  $t \rightarrow \infty$ , indicating the asymptotic convergence of filtered errors to zero.

The control laws  $I_q^*$ ,  $U_q$ ,  $U_d$ , and  $U_{zj}$  for  $j = 1, \dots, 4$  given in (52) to (55), and they may be readily derived if the nonlinear functions  $f_1, \dots, f_4$  and  $g_1, \dots, g_4$  are known; nevertheless, the specific forms of these nonlinear functions remain unidentified. Therefore, seven adaptive fuzzy logic systems are used to directly approach these control laws.

### 5. Overview of the Fuzzy Logic System

A fuzzy logic system is composed of many components: a fuzzifier, a set of fuzzy if-then rules, a fuzzy inference engine, and a defuzzifier. These components are shown in Figure 4.

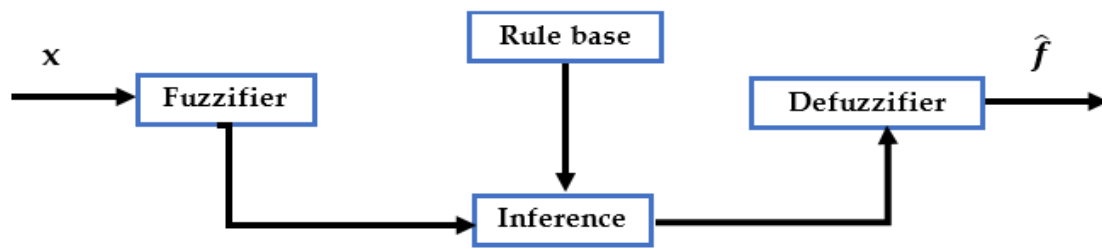


Figure 4. Fuzzy logic system configuration.

The fuzzy inference engine uses fuzzy if-then rules to convert an input vector,  $x^T = [x_1, x_2, \dots, x_n] \in \mathfrak{R}^n$ , to an output,  $\hat{f} \in \mathfrak{R}^n$ . The  $i$ -th fuzzy rule is expressed as follows:

$$\text{Rule (i): if } x_1 \text{ is } B_1^i \text{ and } \dots \text{ and } x_n \text{ is } B_n^i \text{ then } \hat{f} \text{ is } \theta_i \tag{56}$$

where  $B_1^i, B_2^i, \dots, B_n^i$  are fuzzy sets, and  $y_i$  is the fuzzy output singleton in the  $i$ th rule. The Singleton fuzzifier, product inference, and center-average defuzzifier produce the fuzzy system’s output and may be written as:

$$\hat{f}(x) = \frac{\sum_{i=1}^m y_i \left( \prod_{l=1}^n \mu_{B_l^i}(x_l) \right)}{\sum_{i=1}^m \left( \prod_{l=1}^n \mu_{B_l^i}(x_l) \right)} = \Theta^T \psi(x) \tag{57}$$

The degree of membership of  $x_l$  to  $B_l^i$  is denoted as  $\mu_{B_l^i}(x_l)$ . The number of fuzzy rules is represented by  $m$ . The adjustable parameter vector denoted by  $\Theta^T = [\theta_1, \theta_2, \dots, \theta_m]$  is formed by consequent parameters, and the vector  $\psi^T(x) = [\psi_1, \psi_2, \dots, \psi_m]$  with the following:

$$\psi_i(x) = \frac{\left( \prod_{l=1}^n \mu_{B_l^i}(x_l) \right)}{\sum_{i=1}^m \left( \prod_{l=1}^n \mu_{B_l^i}(x_l) \right)} \tag{58}$$

Referring to the fuzzy basis function (FBF), the assumption that the FBFs are chosen in such a manner that there is always at least one active rule is made throughout the whole of the work [10]; that is to say,  $\sum_{i=1}^m \left( \prod_{l=1}^n \mu_{B_l^i}(x_l) \right) > 0$ .

The fuzzy system (57) is often used in control systems. Based on the universal approximation findings [42,43], the fuzzy system (16) has the capability to estimate any nonlinear smooth function,  $f(x)$ , inside a limited working region with a high level of accuracy.

It is crucial to specify the structure of the fuzzy system, including the relevant inputs, the number of membership functions for each input, and the number of rules. Additionally, it is important to accurately define the parameters of the membership functions in advance. The subsequent parameters,  $\Theta$ , are subsequently calculated by suitable adaption methods.

### 6. Model Free Control on Adaptive Fuzzy Control Design for DSPMSM

The goal is to develop an appropriate adaptive fuzzy control system for an uncertain DSPMSM model in order to achieve the precise tracking of torque and speed. Fuzzy logic systems are used to approximate the ideal controls,  $U_{zj}$ , for  $j = 1, \dots, 4, U_q$ , and  $U_d$ .

**Lemma 1 ([10]).** For each real continuous function,  $f(x)$ , defined on a compact subset,  $\Phi_f \subset \mathfrak{R}^n$ , and for any random  $\varepsilon > 0$ , there exists a fuzzy logic system, such that we have the following:

$$\sup_{x \in \Phi_f} \left| f(x) - \Theta^T \psi(x) \right| \leq \varepsilon \tag{59}$$

By utilizing Lemma 1 and referring to the demonstration provided in [10], it can be concluded that fuzzy logic systems possess the ability to universally approximate any smooth function inside a compact set. Given the approximation capacity of fuzzy logic systems, it is reasonable to suppose that the control laws,  $U_{zj}$ , for  $j = 1, \dots, 4$ ,  $I_q^*$ ,  $U_q$ , and  $U_d$  may be estimated as follows:

$$U_{zj}(x_j|\Theta_j) = \Theta_j^T \psi_j(x_j) \text{ for } j = 1, \dots, 4 \tag{60}$$

$$I_q^*(x_5|\Theta_5) = \Theta_5^T \psi_5(x_5) \tag{61}$$

$$U_q(x_6|\Theta_6) = \Theta_6^T \psi_6(x_6) \tag{62}$$

$$U_d(x_7|\Theta_7) = \Theta_7^T \psi_7(x_7) \tag{63}$$

As stated in [29], the optimal parameter vectors,  $\Theta_j^*$ , for  $j = 1, \dots, 4$ ,  $\Theta_5^*$ ,  $\Theta_6^*$ , and  $\Theta_7^*$  are determined as follows:

$$\Theta_j^* = \arg \min_{\Theta_j \in \Phi_{\theta_j}} \left\{ \sup_{x_j \in \Phi_{x_j}} |\hat{U}_{zj}(x_j|\Theta_j) - U_{zj}(t)| \right\} \text{ for } j = 1, \dots, 4 \tag{64}$$

$$\Theta_5^* = \arg \min_{\Theta_5 \in \Phi_{\theta_5}} \left\{ \sup_{x_5 \in \Phi_{x_5}} |I_q^*(x_5|\Theta_5) - I_q^*(t)| \right\} \tag{65}$$

$$\Theta_6^* = \arg \min_{\Theta_6 \in \Phi_{\theta_6}} \left\{ \sup_{x_6 \in \Phi_{x_6}} |\hat{U}_q(x_6|\Theta_6) - U_q(t)| \right\} \tag{66}$$

$$\Theta_7^* = \arg \min_{\Theta_7 \in \Phi_{\theta_7}} \left\{ \sup_{x_7 \in \Phi_{x_7}} |\hat{U}_d(x_7|\Theta_7) - U_d(t)| \right\} \tag{67}$$

where  $\Phi_{x_j}$ ,  $\Phi_{x_5}$ ,  $\Phi_{x_6}$ , and  $\Phi_{x_7}$  are compact set for  $x_j$ ,  $x_5$ ,  $x_6$ , and  $x_7$ . On the other hand,  $\Phi_{\theta_j}$ ,  $\Phi_{\theta_5}$ ,  $\Phi_{\theta_6}$ , and  $\Phi_{\theta_7}$  are compact set for  $\theta_j$ ,  $\theta_5$ ,  $\theta_6$ , and  $\theta_7$ .

Furthermore, the minimal fuzzy approximation errors  $\varepsilon_j$ ,  $\varepsilon_5$ ,  $\varepsilon_6$ , and  $\varepsilon_7$  are precisely specified as follows:

$$\varepsilon_j = U_{zj}(t) - \hat{U}_{zj}(x_j|\Theta_j^*) \text{ for } j = 1, \dots, 4 \tag{68}$$

$$\varepsilon_5 = I_q^*(t) - \hat{I}_q^*(x_5|\Theta_5^*) \tag{69}$$

$$\varepsilon_6 = U_q(t) - \hat{U}_q(x_6|\Theta_6^*) \tag{70}$$

$$\varepsilon_7 = U_d(t) - \hat{U}_d(x_7|\Theta_7^*) \tag{71}$$

The control laws,  $U_{zj}$ , for  $j = 1, \dots, 4$ ,  $I_q^*$ ,  $U_q$ , and  $U_d$  may be reformulated as follows:

$$\begin{aligned} U_{zj}(t) &= \hat{U}_{zj}(x_j|\Theta_j^*) + \varepsilon_j \\ &= \Theta_j^{*T} \psi_j(x_j) + \varepsilon_j \text{ for } j = 1, \dots, 4 \end{aligned} \tag{72}$$

$$\begin{aligned} I_q^*(t) &= \hat{I}_q^*(x_5|\Theta_5^*) + \varepsilon_5 \\ &= \Theta_5^{*T} \psi_5(x_5) + \varepsilon_5 \end{aligned} \tag{73}$$

$$\begin{aligned} U_q(t) &= \hat{U}_q(x_6|\Theta_6^*) + \varepsilon_6 \\ &= \Theta_6^{*T} \psi_6(x_6) + \varepsilon_6 \end{aligned} \tag{74}$$

$$\begin{aligned}
 U_d(t) &= \hat{U}_d(x_7|\Theta_7^*) + \varepsilon_7 \\
 &= \Theta_7^{*T} \psi_7(x_7) + \varepsilon_7
 \end{aligned}
 \tag{75}$$

Let us suppose that the minimal fuzzy approximation errors  $\varepsilon_j$ ,  $\varepsilon_5$ ,  $\varepsilon_6$ , and  $\varepsilon_7$  are, respectively, bounded above by  $\bar{\varepsilon}_j > 0$ ,  $\bar{\varepsilon}_5 > 0$ ,  $\bar{\varepsilon}_6 > 0$ , and  $\bar{\varepsilon}_7 > 0$ , meaning that  $|\bar{\varepsilon}_j| \leq \bar{\varepsilon}_j$ ,  $|\bar{\varepsilon}_5| \leq \bar{\varepsilon}_5$ ,  $|\bar{\varepsilon}_6| \leq \bar{\varepsilon}_6$ , and  $|\bar{\varepsilon}_7| \leq \bar{\varepsilon}_7$ .

### 7. Controller Design

The suggested controller in this section uses fuzzy adaptive backstepping and parameter adaptive laws to ensure that all internal signals of the closed-loop system are uniformly ultimately bounded and to minimize filtered errors given in (31) to (34).

In order to estimate the nonlinear control laws,  $U_{z_j}(t)$ ,  $I_q^*(t)$ ,  $U_q(t)$ , and  $U_d(t)$ , presented in (52) to (55), the fuzzy adaptive control terms in (76) to (79) are defined as  $\hat{U}_{z_j}(t)$ ,  $\hat{I}_q^*(t)$ ,  $\hat{U}_q(t)$ , and  $\hat{U}_d(t)$ :

$$\hat{U}_{z_j}(t) = \Theta_j^T \psi_j(x_j) \tag{76}$$

$$\hat{I}_q^*(t) = \Theta_5^T \psi_5(x_5) \tag{77}$$

$$\hat{U}_q(t) = \Theta_6^T \psi_6(x_6) \tag{78}$$

$$\hat{U}_d(t) = \Theta_7^T \psi_7(x_7) \tag{79}$$

The selected input vectors for the used fuzzy systems are determined as follows:

$$x_j = [i_{z_j}, Z_{i_{z_j}}]^T \text{ for } j = 1, \dots, 4, \quad x_5 = [\Omega, i_q]^T, \quad x_6 = [\Omega, i_q, i_q^*, Z_\Omega]^T, \quad x_7 = [i_d, i_q]^T$$

The adaptive control laws that guarantee the stability of the closed-loop system may be written as follows [28]:

$$V_{z_j}(t) = \hat{U}_{z_j}(t) + \hat{\varepsilon}_j \tanh\left(\frac{S_{z_j}}{\chi_j}\right) + c_{z_j} S_{z_j} \text{ for } j = 1, \dots, 4 \tag{80}$$

$$i_q^* = \hat{I}_q^*(t) + \hat{\varepsilon}_5 \tanh\left(\frac{S_\Omega}{\chi_5}\right) + c_\Omega S_\Omega \tag{81}$$

$$V_q(t) = \hat{U}_q(t) + \hat{\varepsilon}_6 \tanh\left(\frac{S_{i_q}}{\chi_6}\right) + c_{i_q} S_{i_q} \tag{82}$$

$$V_d(t) = \hat{U}_d(t) + \hat{\varepsilon}_7 \tanh\left(\frac{S_{i_d}}{\chi_7}\right) + c_{i_d} S_{i_d} \tag{83}$$

where  $\chi_j, \chi_5, \chi_6$ , and  $\chi_7$  are designed positive constants.

Then,  $\hat{\varepsilon}_j, \hat{\varepsilon}_5, \hat{\varepsilon}_6$ , and  $\hat{\varepsilon}_7$  are adjusted as follows:

$$\dot{\hat{\varepsilon}}_j = \eta_j S_{z_j} \tanh\left(\frac{S_{z_j}}{\chi_j}\right) - \alpha_j \hat{\varepsilon}_j \tag{84}$$

$$\dot{\hat{\varepsilon}}_5 = \eta_5 S_\Omega \tanh\left(\frac{S_\Omega}{\chi_5}\right) - \alpha_5 \hat{\varepsilon}_5 \tag{85}$$

$$\dot{\hat{\varepsilon}}_6 = \eta_6 S_{i_q} \tanh\left(\frac{S_{i_q}}{\chi_6}\right) - \alpha_6 \hat{\varepsilon}_6 \tag{86}$$

$$\dot{\hat{\varepsilon}}_7 = \eta_7 S_{i_d} \tanh\left(\frac{S_{i_d}}{\chi_7}\right) - \alpha_7 \hat{\varepsilon}_7 \tag{87}$$

where  $\eta_j, \eta_5, \eta_6, \eta_7, \alpha_j, \alpha_5, \alpha_6$ , and  $\alpha_7$  are designed positive constants.

The vectors  $\Theta_j, \Theta_5, \Theta_6,$  and  $\Theta_7$  represent the adaptable parameters of the fuzzy logic system and are defined as follows:

$$\dot{\Theta}_j = \gamma_j S_{zj} \psi_j(x_j) - \sigma_j \dot{\Theta}_j \tag{88}$$

$$\dot{\Theta}_5 = \gamma_5 S_{\Omega} \psi_5(x_5) - \sigma_5 \dot{\Theta}_5 \tag{89}$$

$$\dot{\Theta}_6 = \gamma_6 S_{i_q} \psi_6(x_6) - \sigma_6 \dot{\Theta}_6 \tag{90}$$

$$\dot{\Theta}_7 = \gamma_7 S_{i_d} \psi_7(x_7) - \sigma_7 \dot{\Theta}_7 \tag{91}$$

By replacing (76) in (80), (77) in (81), (78) in (82), and (79) in (83), we yield the following:

$$V_{zj}(t) = \Theta_j^T \psi_j(x_j) + \hat{\varepsilon}_j \tanh\left(\frac{S_{zj}}{\chi_j}\right) + c_{zj} S_{zj} \text{ for } j = 1, \dots, 4 \tag{92}$$

$$i_q^* = \Theta_5^T \psi_5(x_5) + \hat{\varepsilon}_5 \tanh\left(\frac{S_{\Omega}}{\chi_5}\right) + c_{\Omega} S_{\Omega} \tag{93}$$

$$U_q(t) = \Theta_6^T \psi_6(x_6) + \hat{\varepsilon}_6 \tanh\left(\frac{S_{i_q}}{\chi_6}\right) + c_{i_q} S_{i_q} \tag{94}$$

$$U_d(t) = \Theta_7^T \psi_7(x_7) + \hat{\varepsilon}_7 \tanh\left(\frac{S_{i_d}}{\chi_7}\right) + c_{i_d} S_{i_d} \tag{95}$$

### 8. Stability Demonstration Using Lyapunov Theory

Given the following candidate Lyapunov function,

$$V = \frac{1}{2} \sum_{j=1}^4 \left( S_{zj}^2 + \frac{1}{\gamma_j} \tilde{\Theta}_j^T \tilde{\Theta}_j + \frac{1}{\eta_j} \tilde{\varepsilon}_j^T \tilde{\varepsilon}_j \right) + \frac{1}{2} \left( S_{\Omega}^2 + \frac{1}{\gamma_5} \tilde{\Theta}_5^T \tilde{\Theta}_5 + \frac{1}{\eta_5} \tilde{\varepsilon}_5^T \tilde{\varepsilon}_5 \right) + \frac{1}{2} \left( S_{i_q}^2 + \frac{1}{\gamma_6} \tilde{\Theta}_6^T \tilde{\Theta}_6 + \frac{1}{\eta_6} \tilde{\varepsilon}_6^T \tilde{\varepsilon}_6 \right) + \frac{1}{2} \left( S_{i_d}^2 + \frac{1}{\gamma_7} \tilde{\Theta}_7^T \tilde{\Theta}_7 + \frac{1}{\eta_7} \tilde{\varepsilon}_7^T \tilde{\varepsilon}_7 \right) \tag{96}$$

where  $\tilde{\Theta}_j, \tilde{\Theta}_5, \tilde{\Theta}_6,$  and  $\tilde{\Theta}_7$  are the approximation errors, which are given as follows:

$$\tilde{\Theta}_j^T = \Theta_j^{T*} - \Theta_j^T \tag{97}$$

$$\tilde{\Theta}_5^T = \Theta_5^{T*} - \Theta_5^T \tag{98}$$

$$\tilde{\Theta}_6^T = \Theta_6^{T*} - \Theta_6^T \tag{99}$$

$$\tilde{\Theta}_7^T = \Theta_7^{T*} - \Theta_7^T \tag{100}$$

$\tilde{\varepsilon}_j, \tilde{\varepsilon}_5, \tilde{\varepsilon}_6,$  and  $\tilde{\varepsilon}_7$  are the approximation errors expressed in (101) to (104), with  $\varepsilon_j^*, \varepsilon_5^*, \varepsilon_6^*$ , and  $\varepsilon_7^*$  serving as the optimal parameters; and  $\hat{\varepsilon}_j, \hat{\varepsilon}_5, \hat{\varepsilon}_6,$  and  $\hat{\varepsilon}_7$  are the estimate of  $\varepsilon_j^*, \varepsilon_5^*, \varepsilon_6^*$ , and  $\varepsilon_7^*$ , respectively.

$$\tilde{\varepsilon}_j = \varepsilon_j^* - \hat{\varepsilon}_j \tag{101}$$

$$\tilde{\varepsilon}_5 = \varepsilon_5^* - \hat{\varepsilon}_5 \tag{102}$$

$$\tilde{\varepsilon}_6 = \varepsilon_6^* - \hat{\varepsilon}_6 \tag{103}$$

$$\tilde{\varepsilon}_7 = \varepsilon_7^* - \hat{\varepsilon}_7 \tag{104}$$

The temporal derivative of  $V$  is computed as follows:

$$\dot{V} = \sum_{j=1}^4 \left( S_{zj} \{U_{zj} - V_{zj}\} + \frac{1}{\gamma_j} \tilde{\Theta}_j^T \tilde{\Theta}_j + \frac{1}{\eta_j} \tilde{\varepsilon}_j^T \tilde{\varepsilon}_j \right) + \left( S_{\Omega} \{I_q^* - i_q^*\} + \frac{1}{\gamma_5} \tilde{\Theta}_5^T \tilde{\Theta}_5 + \frac{1}{\eta_5} \tilde{\varepsilon}_5^T \tilde{\varepsilon}_5 \right) + \left( S_{i_q} \{U_q - V_q\} + \frac{1}{\gamma_6} \tilde{\Theta}_6^T \tilde{\Theta}_6 + \frac{1}{\eta_6} \tilde{\varepsilon}_6^T \tilde{\varepsilon}_6 \right) + \left( S_{i_d} \{U_d - V_d\} + \frac{1}{\gamma_7} \tilde{\Theta}_7^T \tilde{\Theta}_7 + \frac{1}{\eta_7} \tilde{\varepsilon}_7^T \tilde{\varepsilon}_7 \right) \tag{105}$$

By introducing (72) through (75) and (92) through (95) in (105), we can yield the following:

$$\dot{V} = \sum_{j=1}^4 \left( S_{zj} \left\{ \Theta_j^{T*} \psi_j(x_j) + \varepsilon_j - \Theta_j^T \psi_j(x_j) - \hat{\varepsilon}_j \tanh\left(\frac{S_{zj}}{\chi_j}\right) - c_{zj} S_{zj} \right\} + \frac{1}{\gamma_j} \tilde{\Theta}_j^T \tilde{\Theta}_j + \frac{1}{\eta_j} \tilde{\varepsilon}_j^T \tilde{\varepsilon}_j \right) + \left( S_{\Omega} \left\{ \Theta_5^{T*} \psi_5(x_5) + \varepsilon_5 - \Theta_5^T \psi_5(x_5) - \hat{\varepsilon}_5 \tanh\left(\frac{S_{\Omega}}{\chi_5}\right) - c_{\Omega} S_{\Omega} \right\} + \frac{1}{\gamma_5} \tilde{\Theta}_5^T \tilde{\Theta}_5 + \frac{1}{\eta_5} \tilde{\varepsilon}_5^T \tilde{\varepsilon}_5 \right) + \left( S_{i_q} \left\{ \Theta_6^{T*} \psi_6(x_6) + \varepsilon_6 - \Theta_6^T \psi_6(x_6) - \hat{\varepsilon}_6 \tanh\left(\frac{S_{i_q}}{\chi_6}\right) - c_{i_q} S_{i_q} \right\} + \frac{1}{\gamma_6} \tilde{\Theta}_6^T \tilde{\Theta}_6 + \frac{1}{\eta_6} \tilde{\varepsilon}_6^T \tilde{\varepsilon}_6 \right) + \left( S_{i_d} \left\{ \Theta_7^{T*} \psi_7(x_7) + \varepsilon_7 - \Theta_7^T \psi_7(x_7) - \hat{\varepsilon}_7 \tanh\left(\frac{S_{i_d}}{\chi_7}\right) - c_{i_d} S_{i_d} \right\} + \frac{1}{\gamma_7} \tilde{\Theta}_7^T \tilde{\Theta}_7 + \frac{1}{\eta_7} \tilde{\varepsilon}_7^T \tilde{\varepsilon}_7 \right) \tag{106}$$

Given that the optimal parameters  $\Theta_j^{T*}$ ,  $\Theta_5^{T*}$ ,  $\Theta_6^{T*}$ ,  $\Theta_7^{T*}$ ,  $\varepsilon_j^*$ ,  $\varepsilon_5^*$ ,  $\varepsilon_6^*$ , and  $\varepsilon_7^*$  vary slowly over time,  $(\dot{\Theta}_j^{T*} = \dot{\Theta}_5^{T*} = \dot{\Theta}_6^{T*} = \dot{\Theta}_7^{T*} = 0)$  and  $(\dot{\varepsilon}_m^* = \dot{\varepsilon}_5^* = \dot{\varepsilon}_6^* = \dot{\varepsilon}_7^* = 0)$ , the temporal derivative of the approximation errors may be expressed as follows:

$$\begin{cases} \dot{\tilde{\Theta}}_j^T = -\dot{\Theta}_j^T \\ \dot{\tilde{\Theta}}_5^T = -\dot{\Theta}_5^T \\ \dot{\tilde{\Theta}}_6^T = -\dot{\Theta}_6^T \\ \dot{\tilde{\Theta}}_7^T = -\dot{\Theta}_7^T \end{cases} \tag{107}$$

$$\begin{cases} \dot{\tilde{\varepsilon}}_j = -\dot{\varepsilon}_j \\ \dot{\tilde{\varepsilon}}_5 = -\dot{\varepsilon}_5 \\ \dot{\tilde{\varepsilon}}_6 = -\dot{\varepsilon}_6 \\ \dot{\tilde{\varepsilon}}_7 = -\dot{\varepsilon}_7 \end{cases} \tag{108}$$

By substituting (107) and (108) into (106), we obtain the following:

$$\dot{V} = \sum_{j=1}^4 \left( -c_{zj} S_{zj}^2 + S_{zj} \tilde{\Theta}_j^T \psi_j(x_j) + S_{zj} \left\{ \varepsilon_j - \hat{\varepsilon}_j \tanh\left(\frac{S_{zj}}{\chi_j}\right) \right\} - \frac{1}{\gamma_j} \tilde{\Theta}_j^T \dot{\tilde{\Theta}}_j + \frac{1}{\eta_j} \tilde{\varepsilon}_j^T \dot{\tilde{\varepsilon}}_j \right) + \left( -c_{\Omega} S_{\Omega}^2 + S_{\Omega} \tilde{\Theta}_5^T \psi_5(x_5) + S_{\Omega} \left\{ \varepsilon_5 - \hat{\varepsilon}_5 \tanh\left(\frac{S_{\Omega}}{\chi_5}\right) \right\} - \frac{1}{\gamma_5} \tilde{\Theta}_5^T \dot{\tilde{\Theta}}_5 + \frac{1}{\eta_5} \tilde{\varepsilon}_5^T \dot{\tilde{\varepsilon}}_5 \right) + \left( -c_{i_q} S_{i_q}^2 + S_{i_q} \tilde{\Theta}_6^T \psi_6(x_6) + S_{i_q} \left\{ \varepsilon_6 - \hat{\varepsilon}_6 \tanh\left(\frac{S_{i_q}}{\chi_6}\right) \right\} - \frac{1}{\gamma_6} \tilde{\Theta}_6^T \dot{\tilde{\Theta}}_6 + \frac{1}{\eta_6} \tilde{\varepsilon}_6^T \dot{\tilde{\varepsilon}}_6 \right) + \left( S_{i_d} \left\{ \Theta_7^{T*} \psi_7(x_7) + \varepsilon_7 - \Theta_7^T \psi_7(x_7) - \hat{\varepsilon}_7 \tanh\left(\frac{S_{i_d}}{\chi_7}\right) - c_{i_d} S_{i_d} \right\} + \frac{1}{\gamma_7} \tilde{\Theta}_7^T \dot{\tilde{\Theta}}_7 + \frac{1}{\eta_7} \tilde{\varepsilon}_7^T \dot{\tilde{\varepsilon}}_7 \right) \tag{109}$$

$$\begin{aligned}
 \dot{V} \leq & \sum_{j=1}^4 \left( -c_{zj} S_{zj}^2 + \frac{1}{\gamma_j} \tilde{\Theta}_j^T \left\{ \gamma_j S_{zj} \psi_j(x_j) - \dot{\Theta}_j \right\} + |S_{zj}| \varepsilon_j^* - S_{zj} \hat{\varepsilon}_j \tanh\left(\frac{S_{zj}}{\chi_j}\right) + \frac{1}{\eta_j} \tilde{\varepsilon}_j \left\{ \eta_j S_{zj} \tanh\left(\frac{S_{zj}}{\chi_j}\right) - \dot{\varepsilon}_j \right\} \right. \\
 & \left. - \varepsilon_j^* S_{zj} \tanh\left(\frac{S_{zj}}{\chi_j}\right) + \hat{\varepsilon}_j S_{zj} \tanh\left(\frac{S_{zj}}{\chi_j}\right) \right) + \left( -c_{\Omega} S_{\Omega}^2 + \frac{1}{\gamma_5} \tilde{\Theta}_5^T \left\{ \gamma_5 S_{\Omega} \psi_5(x_5) - \dot{\Theta}_5 \right\} + |S_{\Omega}| \varepsilon_5^* \right. \\
 & \left. - S_{\Omega} \hat{\varepsilon}_5 \tanh\left(\frac{S_{\Omega}}{\chi_5}\right) + \frac{1}{\eta_5} \tilde{\varepsilon}_5 \left\{ \eta_5 S_{\Omega} \tanh\left(\frac{S_{\Omega}}{\chi_5}\right) - \dot{\varepsilon}_5 \right\} - \varepsilon_5^* S_{\Omega} \tanh\left(\frac{S_{\Omega}}{\chi_5}\right) + \hat{\varepsilon}_5 S_{\Omega} \tanh\left(\frac{S_{\Omega}}{\chi_5}\right) \right) \\
 & + \left( -c_{i_q} S_{i_q}^2 + \frac{1}{\gamma_6} \tilde{\Theta}_6^T \left\{ \gamma_6 S_{i_q} \psi_6(x_6) - \dot{\Theta}_6 \right\} + |S_{i_q}| \varepsilon_6^* - S_{i_q} \hat{\varepsilon}_6 \tanh\left(\frac{S_{i_q}}{\chi_6}\right) \right. \\
 & \left. + \frac{1}{\eta_6} \tilde{\varepsilon}_6 \left\{ \eta_6 S_{i_q} \tanh\left(\frac{S_{i_q}}{\chi_6}\right) - \dot{\varepsilon}_6 \right\} - \varepsilon_6^* S_{i_q} \tanh\left(\frac{S_{i_q}}{\chi_6}\right) + \hat{\varepsilon}_6 S_{i_q} \tanh\left(\frac{S_{i_q}}{\chi_6}\right) \right) \\
 & + \left( -c_{i_d} S_{i_d}^2 + \frac{1}{\gamma_7} \tilde{\Theta}_7^T \left\{ \gamma_7 S_{i_d} \psi_7(x_7) - \dot{\Theta}_7 \right\} + |S_{i_d}| \varepsilon_7^* - S_{i_d} \hat{\varepsilon}_7 \tanh\left(\frac{S_{i_d}}{\chi_7}\right) \right. \\
 & \left. + \frac{1}{\eta_7} \tilde{\varepsilon}_7 \left\{ \eta_7 S_{i_d} \tanh\left(\frac{S_{i_d}}{\chi_7}\right) - \dot{\varepsilon}_7 \right\} - \varepsilon_7^* S_{i_d} \tanh\left(\frac{S_{i_d}}{\chi_7}\right) + \hat{\varepsilon}_7 S_{i_d} \tanh\left(\frac{S_{i_d}}{\chi_7}\right) \right)
 \end{aligned} \tag{110}$$

**Lemma 2** ([43]). *The hyperbolic tangent function fulfils the following condition for all given values of  $x \in \mathfrak{R}$  and  $\chi > 0$ :*

$$f(x) = |x| - x \tanh\left(\frac{x}{\chi}\right) \leq \zeta \chi \tag{111}$$

where  $\zeta = 0.2785$ .

By replacing the adaptive rules (84) through (91) into Equation (110) and using Lemma 2, we obtain the following:

$$\begin{aligned}
 \dot{V} \leq & \sum_{j=1}^4 \left( -c_{zj} S_{zj}^2 + \varepsilon_j^* \zeta + \frac{\sigma_j}{\gamma_j} \tilde{\Theta}_j^T \Theta_j + \frac{\alpha_j}{\eta_j} \tilde{\varepsilon}_j \hat{\varepsilon}_j \right) + \left( -c_{\Omega} S_{\Omega}^2 + \varepsilon_5^* \zeta + \frac{\sigma_5}{\gamma_5} \tilde{\Theta}_5^T \Theta_5 + \frac{\alpha_5}{\eta_5} \tilde{\varepsilon}_5 \hat{\varepsilon}_5 \right) + \\
 & \left( -c_{i_q} S_{i_q}^2 + \varepsilon_6^* \zeta + \frac{\sigma_6}{\gamma_6} \tilde{\Theta}_6^T \Theta_6 + \frac{\alpha_6}{\eta_6} \tilde{\varepsilon}_6 \hat{\varepsilon}_6 \right) + \left( -c_{i_d} S_{i_d}^2 + \varepsilon_7^* \zeta + \frac{\sigma_7}{\gamma_7} \tilde{\Theta}_7^T \Theta_7 + \frac{\alpha_7}{\eta_7} \tilde{\varepsilon}_7 \hat{\varepsilon}_7 \right)
 \end{aligned} \tag{112}$$

The following inequalities are derived by replacing Young’s inequality for the terms

$$\frac{\sigma_j}{\gamma_j} \tilde{\Theta}_j^T \Theta_j, \frac{\sigma_5}{\gamma_5} \tilde{\Theta}_5^T \Theta_5, \frac{\sigma_6}{\gamma_6} \tilde{\Theta}_6^T \Theta_6, \frac{\sigma_7}{\gamma_7} \tilde{\Theta}_7^T \Theta_7, \frac{\alpha_j}{\eta_j} \tilde{\varepsilon}_j \hat{\varepsilon}_j, \frac{\alpha_5}{\eta_5} \tilde{\varepsilon}_5 \hat{\varepsilon}_5, \frac{\alpha_6}{\eta_6} \tilde{\varepsilon}_6 \hat{\varepsilon}_6, \text{ and } \frac{\alpha_7}{\eta_7} \tilde{\varepsilon}_7 \hat{\varepsilon}_7 :$$

$$\left\{ \begin{aligned}
 \frac{\sigma_j}{\gamma_j} \tilde{\Theta}_j^T \Theta_j & \leq -\frac{\sigma_j}{2\gamma_j} \tilde{\Theta}_j^T \tilde{\Theta}_j + \frac{\sigma_j}{2\gamma_j} \tilde{\Theta}_j^{T*} \tilde{\Theta}_j^{**} \\
 \frac{\sigma_5}{\gamma_5} \tilde{\Theta}_5^T \Theta_5 & \leq -\frac{\sigma_5}{2\gamma_5} \tilde{\Theta}_5^T \tilde{\Theta}_5 + \frac{\sigma_5}{2\gamma_5} \tilde{\Theta}_5^{T*} \tilde{\Theta}_5^{**} \\
 \frac{\sigma_6}{\gamma_6} \tilde{\Theta}_6^T \Theta_6 & \leq -\frac{\sigma_6}{2\gamma_6} \tilde{\Theta}_6^T \tilde{\Theta}_6 + \frac{\sigma_6}{2\gamma_6} \tilde{\Theta}_6^{T*} \tilde{\Theta}_6^{**} \\
 \frac{\sigma_7}{\gamma_7} \tilde{\Theta}_7^T \Theta_7 & \leq -\frac{\sigma_7}{2\gamma_7} \tilde{\Theta}_7^T \tilde{\Theta}_7 + \frac{\sigma_7}{2\gamma_7} \tilde{\Theta}_7^{T*} \tilde{\Theta}_7^{**}
 \end{aligned} \right. \tag{113}$$

$$\left\{ \begin{aligned}
 \frac{\alpha_j}{\eta_j} \tilde{\varepsilon}_j \hat{\varepsilon}_j & \leq -\frac{\alpha_j}{2\eta_j} \tilde{\varepsilon}_j^2 + \frac{\alpha_j}{2\eta_j} |\varepsilon_j^*|^2 \\
 \frac{\alpha_5}{\eta_5} \tilde{\varepsilon}_5 \hat{\varepsilon}_5 & \leq -\frac{\alpha_5}{2\eta_5} \tilde{\varepsilon}_5^2 + \frac{\alpha_5}{2\eta_5} |\varepsilon_5^*|^2 \\
 \frac{\alpha_6}{\eta_6} \tilde{\varepsilon}_6 \hat{\varepsilon}_6 & \leq -\frac{\alpha_6}{2\eta_6} \tilde{\varepsilon}_6^2 + \frac{\alpha_6}{2\eta_6} |\varepsilon_6^*|^2 \\
 \frac{\alpha_7}{\eta_7} \tilde{\varepsilon}_7 \hat{\varepsilon}_7 & \leq -\frac{\alpha_7}{2\eta_7} \tilde{\varepsilon}_7^2 + \frac{\alpha_7}{2\eta_7} |\varepsilon_7^*|^2
 \end{aligned} \right. \tag{114}$$

Consequently, we may restructure (112) in the following manner:

$$\begin{aligned} \dot{V} \leq & \sum_{j=1}^4 \left( -c_{zj} S_{zj}^2 - \frac{\sigma_j}{2\gamma_j} \tilde{\Theta}_j^T \tilde{\Theta}_j + \frac{\sigma_j}{2\gamma_j} \Theta_j^{T*} \Theta_j^* - \frac{\alpha_j}{2\eta_j} \tilde{\varepsilon}_j^2 + \frac{\alpha_j}{2\eta_j} |\varepsilon_j^*|^2 + \varepsilon_j^* \zeta \right) + \left( -c_{\Omega} S_{\Omega}^2 - \frac{\sigma_5}{2\gamma_5} \tilde{\Theta}_5^T \tilde{\Theta}_5 + \frac{\sigma_5}{2\gamma_5} \Theta_5^{T*} \Theta_5^* \right. \\ & \left. - \frac{\alpha_5}{2\eta_5} \tilde{\varepsilon}_5^2 + \frac{\alpha_5}{2\eta_5} |\varepsilon_5^*|^2 + \varepsilon_5^* \zeta \right) \\ & + \left( -c_{i_q} S_{i_q}^2 - \frac{\sigma_6}{2\gamma_6} \tilde{\Theta}_6^T \tilde{\Theta}_6 + \frac{\sigma_6}{2\gamma_6} \Theta_6^{T*} \Theta_6^* - \frac{\alpha_6}{2\eta_6} \tilde{\varepsilon}_6^2 + \frac{\alpha_6}{2\eta_6} |\varepsilon_6^*|^2 + \varepsilon_6^* \zeta \right) \\ & + \left( -c_{i_d} S_{i_d}^2 - \frac{\sigma_7}{2\gamma_7} \tilde{\Theta}_7^T \tilde{\Theta}_7 + \frac{\sigma_7}{2\gamma_7} \Theta_7^{T*} \Theta_7^* - \frac{\alpha_7}{2\eta_7} \tilde{\varepsilon}_7^2 + \frac{\alpha_7}{2\eta_7} |\varepsilon_7^*|^2 + \varepsilon_7^* \zeta \right) \end{aligned} \tag{115}$$

Let us define

$$\vartheta = \min \left\{ \sigma_j, \alpha_j, 2c_{zj}, \sigma_5, \alpha_5, 2c_{\Omega}, \sigma_6, \alpha_6, 2c_{i_q}, \sigma_7, \alpha_7, 2c_{i_d} \right\} \tag{116}$$

Then, (115) is transformed into the following:

$$\dot{V} \leq -\vartheta V + \rho \tag{117}$$

where

$$\begin{aligned} \rho = & \sum_{j=1}^4 \left( \frac{\sigma_j}{2\gamma_j} \Theta_j^{T*} \Theta_j^* + \frac{\alpha_j}{2\eta_j} |\varepsilon_j^*|^2 + \varepsilon_j^* \zeta \right) + \left( \frac{\sigma_5}{2\gamma_5} \Theta_5^{T*} \Theta_5^* + \frac{\alpha_5}{2\eta_5} |\varepsilon_5^*|^2 + \varepsilon_5^* \zeta \right) + \left( \frac{\sigma_6}{2\gamma_6} \Theta_6^{T*} \Theta_6^* + \frac{\alpha_6}{2\eta_6} |\varepsilon_6^*|^2 + \varepsilon_6^* \zeta \right) \\ & + \left( \frac{\sigma_7}{2\gamma_7} \Theta_7^{T*} \Theta_7^* + \frac{\alpha_7}{2\eta_7} |\varepsilon_7^*|^2 + \varepsilon_7^* \zeta \right) \end{aligned} \tag{118}$$

We can now establish the following theorem, which demonstrates our primary finding in this study.

**Theorem 1.** Consider the six-phase PMSM nonlinear system in (28). Assuming that the previously specified Assumption 1, Assumption 2, and Lemma 1 are correct, the control laws described by Equations (92) through (95), which use adaptive fuzzy logic system, in conjunction with the parameter adaption law detailed in Equations (84) through (91), guarantee that all signals inside the closed-loop system demonstrate uniformly ultimately bounded (UUB) stability. Additionally, the output tracking error is shown to converge to a narrow area in close proximity to the origin. Furthermore, the developed controller has the ability to maintain stability.

**Proof.** The integral of (117) over  $[0, t]$  yields the following result:

$$V(t) \leq V(0) e^{-\vartheta t} + \frac{\rho}{\vartheta} \tag{119}$$

The inequalities represented by (117) suggest that  $V \geq \frac{\rho}{\vartheta}$ ,  $\dot{V} \leq 0$ . Therefore, by utilizing the Lyapunov theorem, the signals  $S_{\Omega}, S_{i_q}, S_{i_d}, S_{zj}, \tilde{\Theta}_j, \tilde{\Theta}_5, \tilde{\Theta}_6, \tilde{\Theta}_7, \tilde{\varepsilon}_j, \tilde{\varepsilon}_5, \tilde{\varepsilon}_6, \tilde{\varepsilon}_7, V_{zj}, i_q^*, V_q$ , and  $V_d$  in the closed-loop systems are bounded. Furthermore, it can be shown that, for any  $Y \geq \sqrt{\frac{\rho}{\vartheta}}$ , there exists a constant  $T > 0$ , such that  $|Z_{\Omega}| \leq Y, |Z_{i_q}| \leq Y, |Z_{i_d}| \leq Y$ , and  $|Z_{i_{zj}}| \leq Y$  for all  $t \geq T$ .

To attain convergence of the tracking error to a small vicinity around zero and minimize  $\sqrt{\frac{\rho}{\vartheta}}$  to the desired extent, it is imperative to select the design parameters  $\eta_j, \eta_5, \eta_6, \eta_7, \gamma_j, \gamma_5, \gamma_6, \gamma_7, \chi_j, \chi_5, \chi_6, \chi_7, \alpha_j, \alpha_5, \alpha_6, \alpha_7, \sigma_j, \sigma_5, \sigma_6, \sigma_7, c_{zj}, c_{\Omega}, c_{i_q}$ , and  $c_{i_d}$  judiciously. Therefore, it is evident that  $\lim_{t \rightarrow \infty} |Z_{\Omega}| \leq Y, \lim_{t \rightarrow \infty} |Z_{i_q}| \leq Y, \lim_{t \rightarrow \infty} |Z_{i_d}| \leq Y$ , and  $\lim_{t \rightarrow \infty} |Z_{i_{zj}}| \leq Y$ . The proof is now concluded.  $\square$

The modification terms  $\alpha_j, \alpha_5, \alpha_6, \alpha_7, \sigma_j, \sigma_5, \sigma_6,$  and  $\sigma_7$  were introduced in the adaptive laws (84) through (91) in order to prevent parameter drift from approximation errors. After modifying adaptive laws, the time derivative of the Lyapunov function utilized for analysis turns negative when parameter estimations surpass specified limitations [44].

Once the control law was established and the system stability was theoretically confirmed, we proposed a system structure for study, as illustrated in Figure 5, incorporating the developed control law, to subject the system to a series of tests.

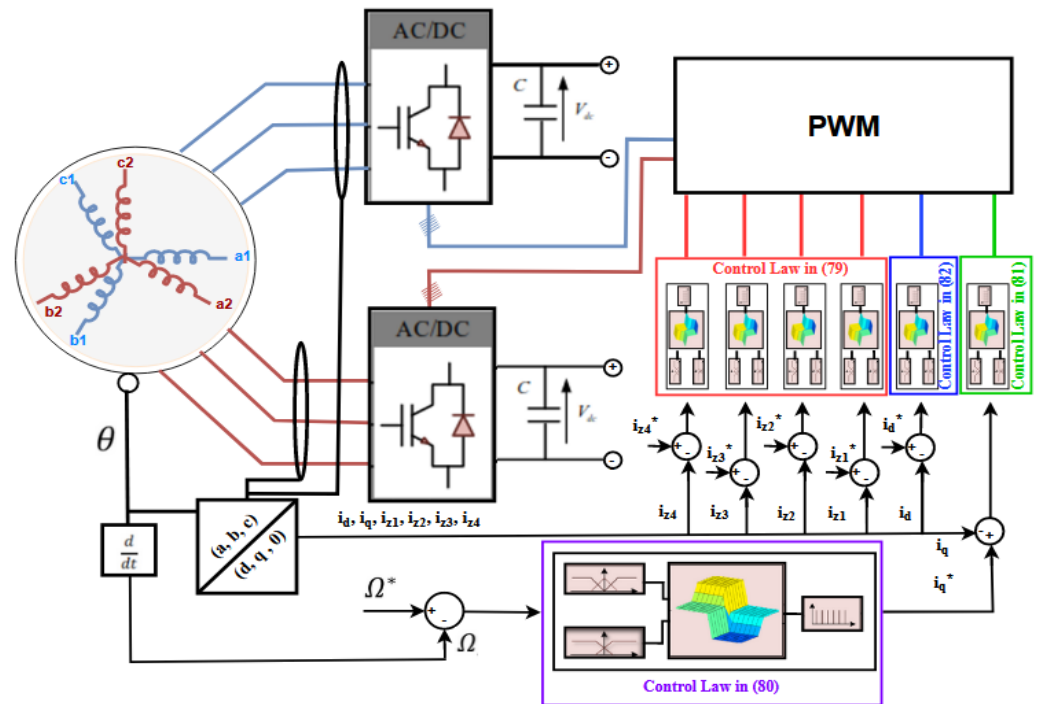


Figure 5. Control architecture of the DSPMSM.

**Remark 1.** A comparative analysis is carried out in Table 1 to provide the greatest visibility and demonstrate the efficacy of the suggested control technique in relation to other relevant works.

Table 1. Control techniques comparison.

Our Control Scheme	Other Approaches	Corresponding Papers
Uncertainty information is not required since the controller updates online to counteract the impact of uncertainty.	Information on uncertainty models is required.	[30–34]
There is no need for an approximation for disturbance since it was addressed conceptually by mathematical procedures, saving the time required for the approximation.	Disturbance was characterized as an external neutral stable system, or it was estimated. The authors considered that the time derivative of the disturbances must be limited.	[35–37]
Control gain is treated as an unknown nonlinear function.	The control gain is a straightforward constant, which restricts the scope of the systems that are taken into consideration.	[38,39]
The closed-loop system exhibits uniform ultimate bounded (UUB) stability, and the tracking error converges exponentially to the origin. This is achieved through the accurate approximation using fuzzy systems and the robust control term based on the tangent hyperbolic function, which effectively handles the residual terms from the fuzzy systems.	The closed-loop system exhibits stability, with the tracking error converging exponentially to a limited set. This behavior is attributed to the presence of residue terms resulting from the approximation.	[35,36,40]

### 9. Real Times Validation Results

To validate and assess the robustness of our control law, which consists of an adaptive fuzzy logic, within the framework of our research in developing control systems for the DSPMSM, we chose to use the RT-LAB platform from OPAL-RT due to its advanced features and effective integration of the hardware-in-the-loop (HIL) approach (Figure 6). By adopting this approach, we were able to combine our complex simulation models with real hardware components, allowing us to validate our designs under conditions close to reality. To demonstrate the robustness of our control, we chose to subject the system to a series of tests. Initially, we varied the control variables, namely the electromagnetic torque and the rotational speed. Subsequently, we made variations in the electrical parameters of the machine during its operation, including doubling the value of the stator resistance and halving the machine’s inductance. Finally, we adjusted the mechanical parameters of the machine, such as inertia and viscous friction, by doubling their nominal values. The nominal parameters of the machine are provided in Table 2.

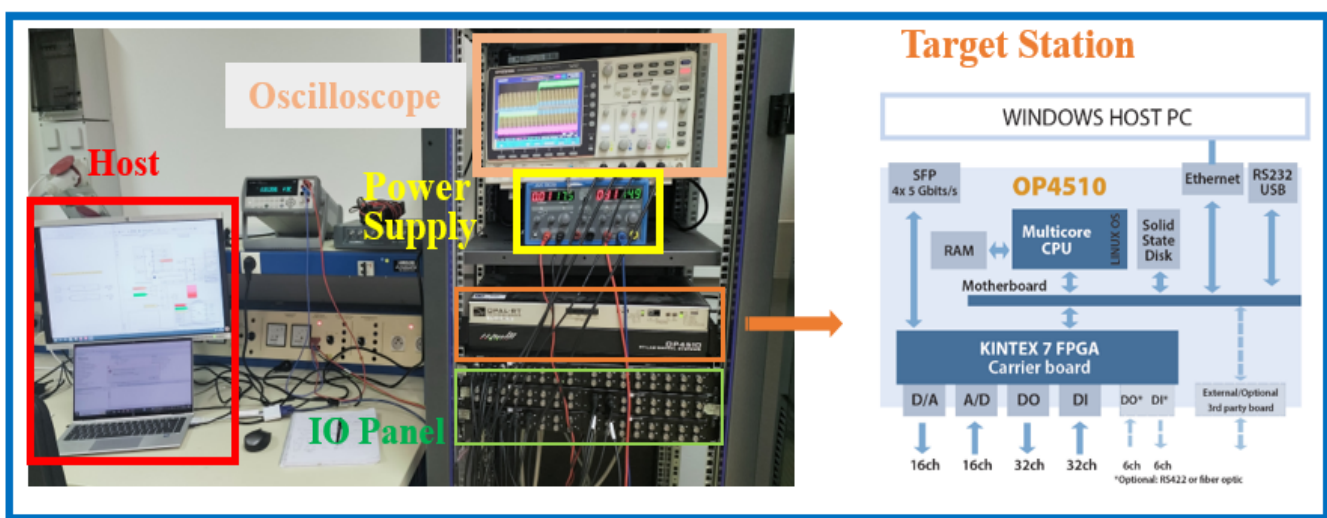


Figure 6. Test bench used for validation test.

Table 2. Machine parameters.

Parameters	Values
Stator resistance $R_s$ (Ohm)	2
Leakage inductance $l_{fs}$ (H)	$0.562 \times 10^{-3}$
Maximum mutual inductance between two stator’s windings $M_{ss}$ (H)	$3.373 \times 10^{-3}$
Rotor flux (Wb)	0.42
Moment of inertia (kg·m <sup>2</sup> )	0.025
Numbers of pole pairs	6
Coefficient of viscose friction (N·m·s/rd)	0.01

The tests carried out to confirm the robustness of the developed control method took place in three following scenarios:

- Scenario 1: variation in operating references;
- Scenario 2: variation in electrical parameters of the DSPMSM;
- Scenario 3: variation in mechanical parameters of the DSPMSM.

#### 9.1. Variation in Operating References

In this section, the references for both the torque and speed of the machine vary over time, and we will examine the behavior of the adopted control approach. At the beginning of operation, between  $t = 0$  and  $t = 3$  s, the applied speed reference is 300 rpm, and from 3 s onwards, the reference transitions to its nominal value of 400 rpm. Similarly,

the electromagnetic torque reference is 60 Nm, and from  $t = 6$  s onwards, the reference transitions to its nominal value of 93.5 Nm.

Figure 7a illustrates the curves of torque and velocity during a variation in their respective setpoints. The setpoint for the load torque is applied at  $t = 6$  s, while that for velocity is set at  $t = 3$  s. It is observed that the torque rigorously follows the setpoint with almost no oscillation. However, an undershoot is noticed during the velocity setpoint change. The integrated fuzzy logic controller quickly brings the system back to its setpoint within just 0.5 s. As for velocity, it reaches its reference after slight oscillations during startup and load torque setpoint changes, but these are promptly corrected by the controller in place, demonstrating high dynamic performance.

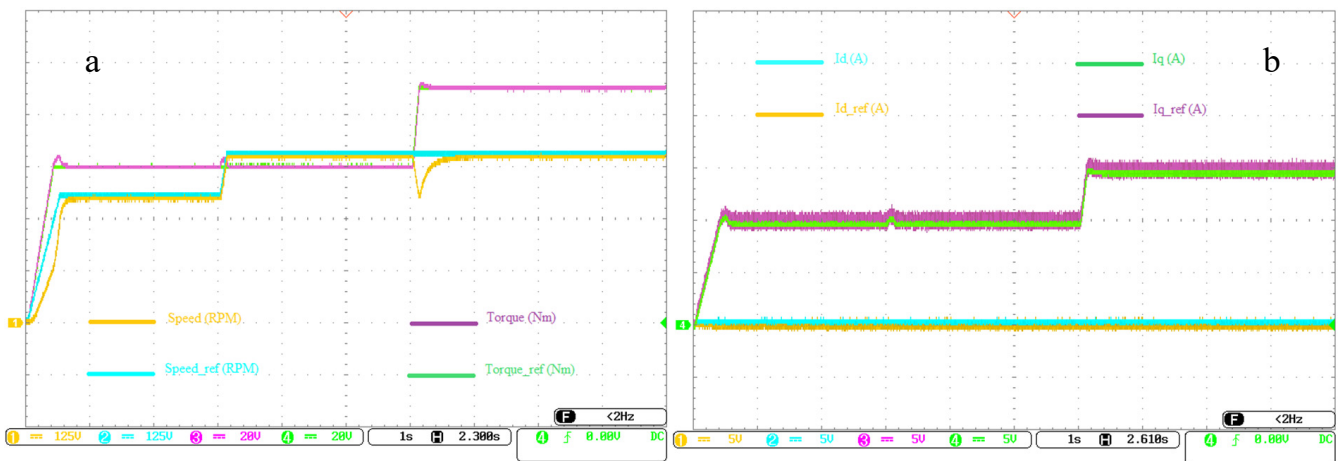


**Figure 7.** (a) Speed and torque curves, and (b) id and iq current curves for operating references variation.

The curves obtained during current regulation in the (d,q,o) plane are presented in Figure 7b. The  $i_d$  current precisely tracks its setpoint, maintained at zero in this selected control mode. Furthermore, the  $i_q$  current also follows its reference, calculated based on the velocity through torque.

The Figure 8 illustrates the variation in the current in the first phase of the first star, as well as the first phase of the second star, with a zoom-in look at the current behavior at the moment when the electromagnetic torque changes from 60 Nm to 93 Nm. It should be noted that, at this moment, the current amplitudes increase from 7 A to 10 A.

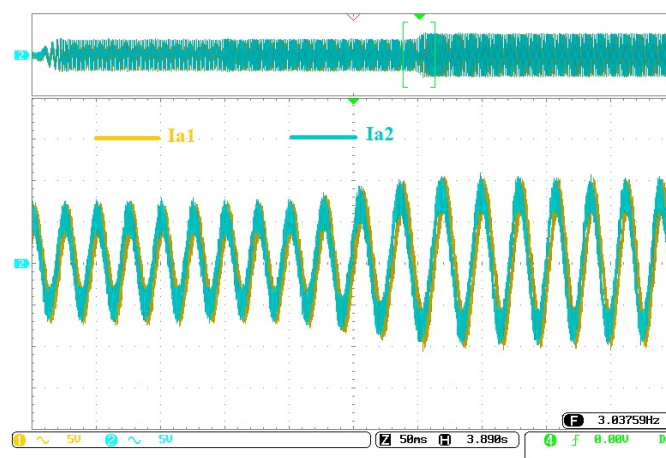


**Figure 8.** ia1 current curves and ia2 current curves for operating references variation.

The currents of the first phase (ia1 and ia2) for the two stator windings of the two stars of the machine are illustrated in Figure 9a. In Figure 9b, the currents of the first phase (ia1 and ia2) and those of the second phase (ib1 and ib2) of the two windings of the two stars of the machine are presented. These current curves exhibit a sinusoidal shape, with a  $30^\circ$  phase shift between the currents of the two stars, in accordance with the electrical and mechanical angle of the machine. However, due to the limitations of the oscilloscope used, only the currents of a few phases are represented, as it has only four acquisition channels.

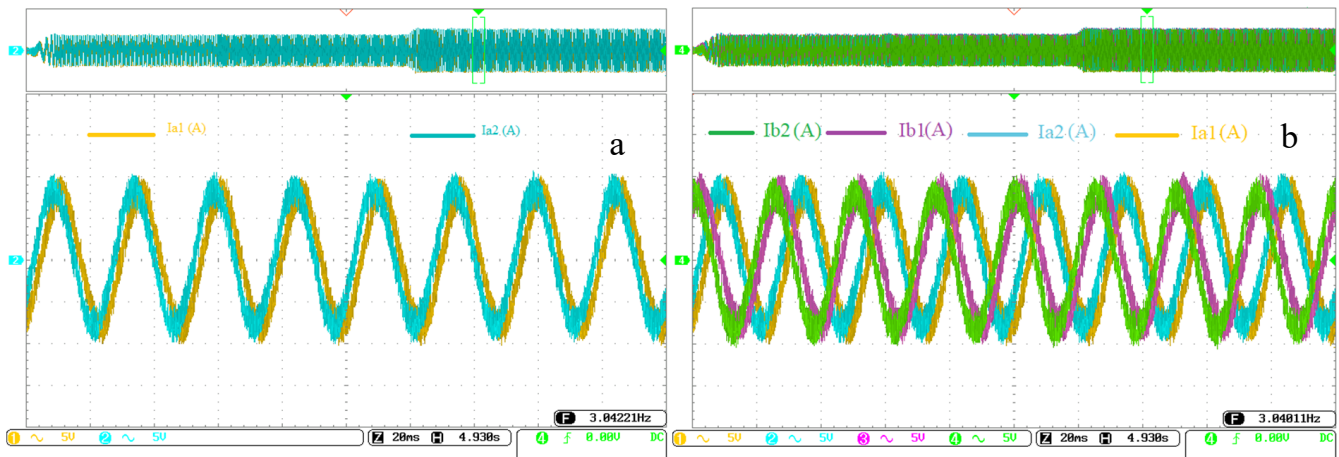


**Figure 9.** (a) ia1 current curves and ia2 current curves; (b) ia1, ia2, ib1, and ib2 current curves for operating references variation.

## 9.2. Variation in Electrical Parameters of DSPMSM

Now, we address the scenario where the electrical parameters of the machine vary (resistance and inductance). We subjected our system to the test by increasing the resistance value from its nominal value, which was 2 ohms until  $t = 3$  s, to 4 ohms, representing a 100% increase. Then, starting from  $t = 6$  s, we reduced the machine's inductance value by 50% compared to its nominal value, which was held constant between  $t = 0$  and  $t = 6$  s. The curves depicting the physical quantities of the machine are shown in the following figures:

In this second case study, which presents the parametric variations in the electrical quantities of the machine, notably the resistance and inductance values, altered by several possible reasons, we can cite some of them: temperature variation within the machine; aging effects; mechanical effects, such as vibrations and shocks; and wear of the stator windings of the machine, as well as the presence of contaminants, can also influence the electrical properties of the materials of the machine, among other things.

Despite the presence of these parametric disturbances of the machine, we observe that the robustness and performance of our system are maintained thanks to the new control technique proposed in this article, which consists of an adaptive fuzzy controller, allowing us to find and readjust the parameters of the regulator to maintain the system at its optimal operating point. These performances are confirmed by the curves presented in Figures 10 and 11. In Figure 10a, the speed shows a slight increase in the overshoot value during startup, but the controller manages to bring the speed value back to its setpoint. Additionally, for the load torque and the id and iq currents, represented in Figure 10b, the setpoints are well followed and respected. The robustness of the deployed adaptive fuzzy controller is confirmed by the quality of the stator currents of the machine, which are sinusoidal in shape, like those obtained in the first case, as shown in Figure 11a,b.

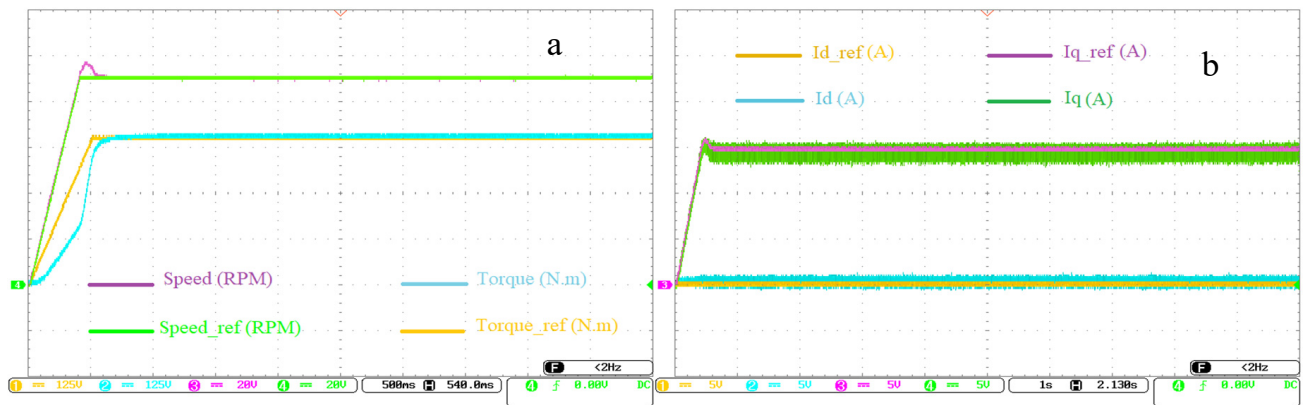


Figure 10. (a) Speed and torque curves, and (b) id and iq current curves for electrical parameters variation.

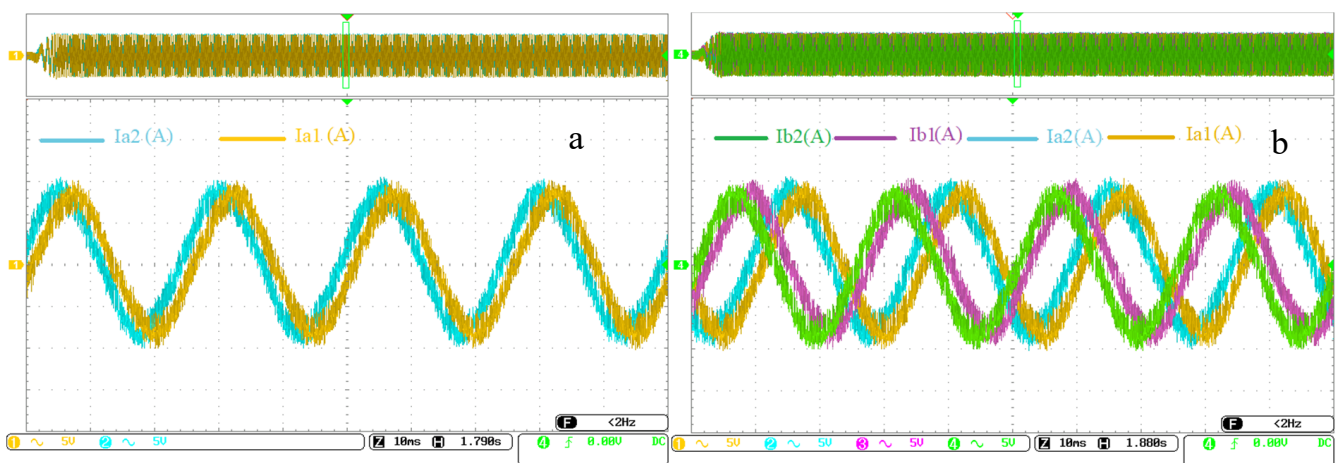


Figure 11. (a) ia1 current curves and ia2 current curves; and (b) ia1, ia2, ib1, and ib2 current curves for electrical parameters variation.

### 9.3. Variation in Mechanical Parameters of DSPMSM

In this new series of tests, we explore variations in the mechanical parameters of the machine, namely inertia and viscous friction. These variations may be due to various factors, such as a coupling issue leading to an increase in the system’s inertia, or problems in the machine’s bearings, resulting in a significant increase in friction. In this section, we examine the impact of these variations by increasing the inertia value to twice its nominal value at  $t = 3$  s, while the friction, initially at its nominal value, is doubled at  $t = 6$  s. The resulting curves from these tests are presented below.

The last case studied concerns the parametric variation in the mechanical quantities of the machine, which may be disturbed by factors such as the mechanical load fluctuations; wear of internal parts, such as bearings and rollers; or lubrication issues with mechanical components. Once again, the robustness of our adaptive fuzzy controller is validated by the maintenance of the machine’s performance despite these disturbances.

Figure 12a shows that the load torque is not affected by the parametric variations, and the id and iq currents, depicted in Figure 12b, also perfectly follow their setpoints. However, a slight increase in the speed overshoot during startup is observed, but the setpoint is quickly reached and followed. The curves in Figure 13a represent two currents: one corresponding to the first phase of the first star, and the other to the first phase of the second star. As for the curves in Figure 13b, they illustrate the currents of the first and second phases of the first star, as well as those of the first and second phases of the second star. These currents maintain a sinusoidal shape, with a peak value close to 10 amperes.

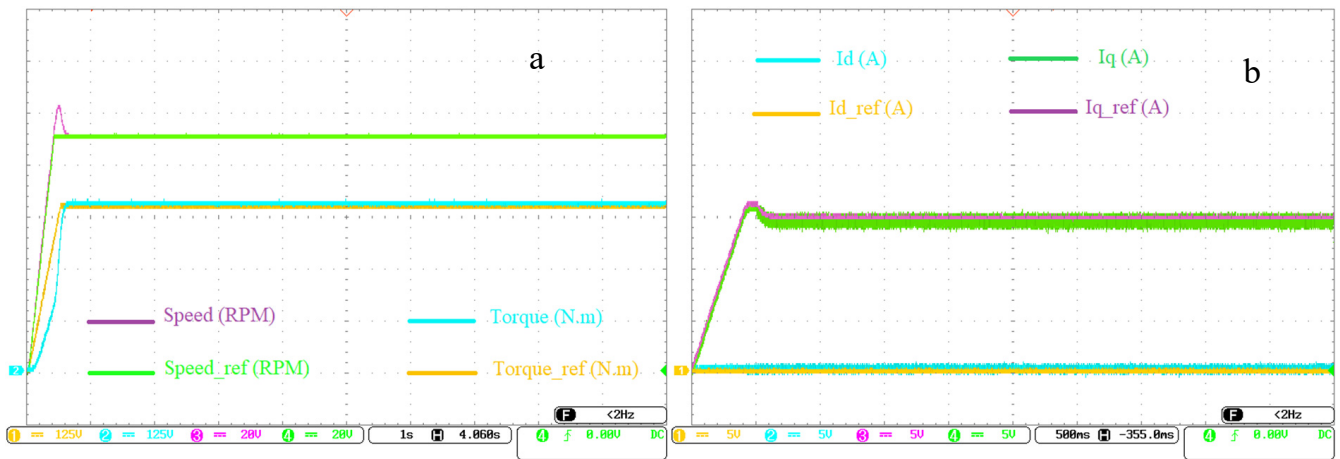


Figure 12. (a) Speed and torque curves, and (b) id and iq current curves for mechanical parameters variation.

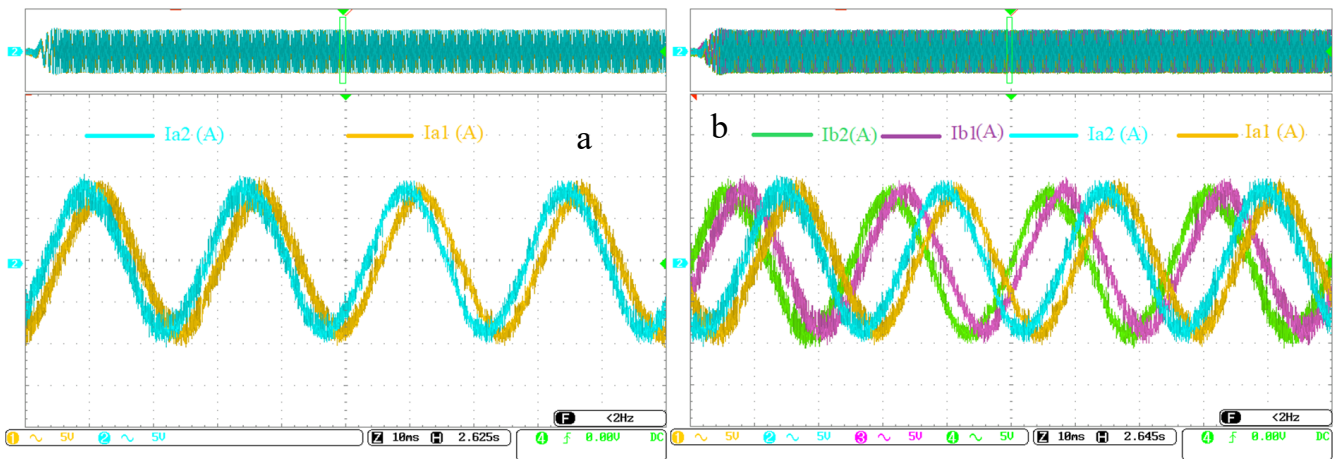


Figure 13. (a) ia1 current curves and ia2 current curves; and (b) ia1, ia2, ib1 and ib2 current curves for mechanical parameters variation.

To make a quantitative comparison between the proposed control method and the controllers proposed in Refs. [30,33], three well-known performance criteria are used. These are the integral of square error (ISE), integral of the absolute value of the error (IAE), and integral of the time multiplied by the absolute value of the error (ITAE). The obtained values for each criterion are summarized in Table 3. It is noted that the proposed control method offers the smallest values control of ISE, IAE, and ITAE as compared to the other two controllers. Hence, it is evident that the suggested controller is optimal and exhibits superior tracking of desired values compared to the other two controllers.

Table 3. Performance indices: ISE, IAE, and ITAE for speed and torque controls.

Control Method	ISE		IAE		ITAE	
	Speed Control	Torque Control	Speed Control	Torque Control	Speed Control	Torque Control
Proposed control in [33]	1.988	$2.141 \times 10^{-2}$	4.387	0.719	3.302	2.821
Proposed control in [30]	1.275	$9.541 \times 10^{-3}$	3.416	0.517	2.782	1.365
Proposed control method	0.813	$5.771 \times 10^{-3}$	2.138	0.365	1.096	0.219

## 10. Conclusions

In this paper, we present a robust fuzzy adaptive control strategy for a DSPMSM, marking a significant advancement in the field of electromechanical system control amidst external disturbances and parametric uncertainties. The methodology developed in this study provides a precise and segmented representation of the system dynamics of the double-star permanent magnet synchronous machine (DSPMSM), achieved through a qualitative analysis and quantitative comparison with recent methods found in the literature. Our qualitative analysis highlighted the characteristics and advantages of our proposed approach, while the quantitative comparison demonstrated its performance and originality. Moreover, by proposing a model of the machine composed of two decoupled sub-models, the first being equivalent to that of a three-phase machine in the Park reference frame, and the second being equivalent to a fourth-order passive circuit, this facilitates the design and implementation of effective control strategies for these machines. Utilizing the Lyapunov function, we successfully developed the algorithm and adaptive parameter law, enabling the reduction of disturbances and parametric uncertainties on the DSPMSM, while maintaining tracking control efficiency and bounded stability in the global closed-loop system. Unlike active disturbance-rejection designs, our suggested technique does not rely on prior knowledge of external disturbances or a mathematical model, thus allowing it to operate optimally even in adverse conditions caused by model errors and nonlinearities. The simulation results consistently demonstrated a high tracking performance, underscoring the robustness and effectiveness of our proposed control method. In the future, our research will focus on improving the performance analysis in more complex scenarios and exploring opportunities to integrate this methodology into various domains of electrical engineering and industrial automation.

**Author Contributions:** Methodology, S.Z.; Validation, D.Z.; Formal analysis, A.D.; Investigation, M.F.B. All authors have read and agreed to the published version of the manuscript.

**Funding:** This research received no external funding.

**Data Availability Statement:** Data is contained within the article.

**Conflicts of Interest:** The authors have no conflicts of interest in this article.

## References

1. Naas, B.; Nezli, L.; Naas, B.; Mahmoudi, M.O.; Elbar, M. Direct Torque Control Based Three Level Inverter-fed Double Star Permanent Magnet Synchronous Machine. *Energy Procedia* **2021**, *18*, 521–530. [[CrossRef](#)]
2. Ziane, D. *Optimisation de la Commande de la Machine Asynchrone Double Etoile en Fonctionnement Normal et Dégradé*; Thèse Université de BEJAIA: Béjaïa, Algeria, 2015; Nantes University: Nantes, France, 2021.
3. Benkhoris, M.F.; Merabtene, M.; Tabar, F.; Davat, B.; Semail, E. Approches de modélisation de la machine synchrone double étoile alimentée par des onduleurs de tension envue de la commande. *Rev. Int. Génie Électrique* **2003**, *6*. [[CrossRef](#)]
4. Naas, B.; Nezli, L.; Elbar, M.; Naas, B. Direct Torque Control of Double Star Synchronous Machine. *Int. J. Recent Trends Eng.* **2009**, *2*, 336.
5. Bojoi, R.; Lazzari, M.; Profumo, F.; Tenconi, A. Digital field-oriented control for dual three-phase induction motor drives. *IEEE Trans. Ind. Appl.* **2003**, *39*, 752–760. [[CrossRef](#)]
6. Zhang, J.-Y.; Zhou, Q.; Wang, K. Dual Three-Phase Permanent Magnet Synchronous Machines Vector Control Based on Triple Rotating Reference Frame. *Energies* **2022**, *15*, 7286. [[CrossRef](#)]
7. Hu, Y.; Zhu, Z.Q.; Odavic, M. Comparison of Two-Individual Current Control and Vector Space. *IEEE Trans. Ind. Appl.* **2017**, *53*, 4483–4492. [[CrossRef](#)]
8. Shu, M.; Ziane, D.; Oukrid, M.; Benkhoris, M.F.; Bernard, N. Dynamic modelling approach in view of vector control and behaviour analysis of multi-three-phase star Permanent Magnet Synchronous Motor drive. *Energies* **2024**, *17*, 1567. [[CrossRef](#)]
9. Laggoun, L.; Youb, L.; Belkacem, S.; Benagougne, S.; Craciunescu, A. Direct torque control using second order Sliding mode of a double star permanent Magnet synchronous machine. In Proceedings of the 4th International Conference on Electrical Engineering and Control Applications, ICEECA 2019, Constantine, Algeria, 17–19 December 2019; pp. 139–153.
10. Wang, L.X. *Adaptive Fuzzy Systems and Control: Design and Stability Analysis*; Prentice-Hall, Inc.: Englewood Cliffs, NJ, USA, 1994.
11. Tong, S.-C.; Li, Y.-M.; Feng, G.; Li, T.-S. Observer-Based Adaptive Fuzzy Backstepping Dynamic Surface Control for a Class of MIMO Nonlinear Systems. *IEEE Trans. Syst. Man Cybern. Part B (Cybern.)* **2011**, *41*, 1124–1135. [[CrossRef](#)] [[PubMed](#)]

12. Lee, H. Robust Adaptive Fuzzy Control by Backstepping for a Class of MIMO Nonlinear Systems. *IEEE Trans. Fuzzy Syst.* **2011**, *19*, 265–275. [[CrossRef](#)]
13. Zhou, Q.; Shi, P.; Lu, J.; Xu, S. Adaptive Output-Feedback Fuzzy Tracking Control for a Class of Nonlinear Systems. *IEEE Trans. Fuzzy Syst.* **2011**, *19*, 972–982. [[CrossRef](#)]
14. Chwa, D. Fuzzy Adaptive Tracking Control of Wheeled Mobile Robots with State-Dependent Kinematic and Dynamic Disturbances. *IEEE Trans. Fuzzy Syst.* **2012**, *20*, 587–593. [[CrossRef](#)]
15. Chen, B.; Liu, X.P.; Ge, S.S.; Lin, C. Adaptive Fuzzy Control of a Class of Nonlinear Systems by Fuzzy Approximation Approach. *IEEE Trans. Fuzzy Syst.* **2012**, *20*, 1012–1021. [[CrossRef](#)]
16. Tong, S.; Li, Y. Adaptive Fuzzy Output Feedback Control of MIMO Nonlinear Systems with Unknown Dead-Zone Inputs. *IEEE Trans. Fuzzy Syst.* **2013**, *21*, 134–146. [[CrossRef](#)]
17. Liu, Z.; Wang, F.; Zhang, Y.; Chen, X.; Chen, C.P. Adaptive Fuzzy Output-Feedback Controller Design for Nonlinear Systems via Backstepping and Small-Gain Approach. *IEEE Trans. Cybern.* **2014**, *44*, 1714–1725. [[CrossRef](#)] [[PubMed](#)]
18. Zhou, Q.; Shi, P.; Xu, S.; Li, H. Adaptive Output Feedback Control for Nonlinear Time-Delay Systems by Fuzzy Approximation Approach. *IEEE Trans. Fuzzy Syst.* **2013**, *21*, 301–313. [[CrossRef](#)]
19. Wang, T.; Zhang, Y.; Qiu, J.; Gao, H. Adaptive Fuzzy Backstepping Control for A Class of Nonlinear Systems with Sampled and Delayed Measurements. *IEEE Trans. Fuzzy Syst.* **2015**, *23*, 302–312. [[CrossRef](#)]
20. Li, Y.; Tong, S.; Liu, Y.; Li, T. Adaptive Fuzzy Robust Output Feedback Control of Nonlinear Systems with Unknown Dead Zones Based on a Small-Gain Approach. *IEEE Trans. Fuzzy Syst.* **2014**, *22*, 164–176. [[CrossRef](#)]
21. Yu, J.; Chen, B.; Yu, H. Fuzzy-approximation-based adaptive control of the chaotic permanent magnet synchronous motor. *Nonlinear Dyn.* **2012**, *69*, 1479–1488. [[CrossRef](#)]
22. Li, Y.; Tong, S.; Li, T. Adaptive fuzzy backstepping control of static var compensator based on state observer. *Nonlinear Dyn.* **2013**, *73*, 133–142. [[CrossRef](#)]
23. Li, Y.; Tong, S.; Li, T. Direct adaptive fuzzy backstepping control of uncertain nonlinear systems in the presence of input saturation. *Neural Comput. Appl.* **2013**, *23*, 1207–1216. [[CrossRef](#)]
24. Li, H.; Li, Z.; Liu, J.; Zheng, X.; Yu, X.; Kaynak, O. Adaptive neural network backstepping control method for aerial manipulator based on coupling disturbance compensation. *J. Frankl. Inst.* **2024**, *361*, 106733. [[CrossRef](#)]
25. Yang, X.; Zhao, Z.; Li, Y.; Yang, G.; Zhao, J.; Liu, H. Adaptive neural network control of manipulators with uncertain kinematics and dynamics. *Eng. Appl. Artif. Intell.* **2024**, *133*, 107935. [[CrossRef](#)]
26. Zhao, N.; Zhao, D.; Liu, Y. Resilient event-triggering adaptive neural network control for networked systems under mixed cyber attacks. *Neural Netw.* **2024**, *174*, 106249. [[CrossRef](#)] [[PubMed](#)]
27. Zhao, D.; Shi, M.; Zhang, H.; Liu, Y.; Zhao, N. Event-triggering adaptive neural network output feedback control for networked systems under false data injection attacks. *Chaos Solitons Fractals* **2024**, *180*, 114584. [[CrossRef](#)]
28. Niu, S.; Wang, J.; Zhao, J.; Shen, W. Neural network-based finite-time command-filtered adaptive backstepping control of electro-hydraulic servo system with a three-stage valve. *ISA Trans.* **2024**, *144*, 419–435. [[CrossRef](#)] [[PubMed](#)]
29. Deng, D.D.; Zhao, X.W.; Lai, Q.; Liu, S. Fuzzy adaptive containment control of non-strict feedback multi-agent systems with prescribed time and accuracy under arbitrary initial conditions. *Inf. Sci.* **2024**, *663*, 120306. [[CrossRef](#)]
30. Rahmatullah, R.; Ak, A.; Serteller, N.F.O. Design of Sliding Mode Control using SVPWM Modulation Method for Speed Control of Induction Motor. *Transp. Res. Procedia* **2023**, *70*, 226–233. [[CrossRef](#)]
31. Zellouma, D.; Bekakra, Y.; Benbouhenni, H. Robust synergetic-sliding mode-based-backstepping control of induction motor with MRAS technique. *Energy Rep.* **2023**, *10*, 3665–3680. [[CrossRef](#)]
32. Rigatos, G.; Abbaszadeh, M.; Sari, B.; Siano, P.; Cuccurullo, G.; Zouari, F. Nonlinear optimal control for a gas compressor driven by an induction motor. *Results Control. Optim.* **2023**, *11*, 100226. [[CrossRef](#)]
33. Zellouma, D.; Bekakra, Y.; Benbouhenni, H. Field-oriented control based on parallel proportional–integral controllers of induction motor drive. *Energy Rep.* **2023**, *9*, 4846–4860. [[CrossRef](#)]
34. Prabhakaran, A.; Ponnusamy, T.; Janarthanan, G. Optimized fractional order PID controller with sensorless speed estimation for torque control in induction motor. *Expert Syst. Appl.* **2024**, *249*, 123574. [[CrossRef](#)]
35. Yoo, K.Y.; Kim, S.; Park, I.; Yoon, H.; Kim, H.S.; Seo, T. Disturbance torque observer-based variable impedance control for compliant stair-descending of transformable wheel mechanism. *Mech. Mach. Theory* **2024**, *194*, 105590. [[CrossRef](#)]
36. Wang, H.; Deng, J.; Zhang, L.; Bao, Q.; Mao, Y. Enhanced disturbance observer-based hybrid cascade active disturbance rejection control design for high-precise tracking system in application to aerospace satellite. *Aerosp. Sci. Technol.* **2024**, *146*, 108939. [[CrossRef](#)]
37. Fu, B.; Che, W.; Wang, Q.; Liu, Y.; Yu, H. Improved sliding-mode control for a class of disturbed systems based on a disturbance observer. *J. Frankl. Inst.* **2024**, *361*, 106699. [[CrossRef](#)]
38. Schuchert, P.; Gupta, V.; Karimi, A. Data-driven fixed-structure frequency-based H<sub>2</sub> and H<sub>∞</sub> controller design. *Automatica* **2024**, *160*, 111398. [[CrossRef](#)]
39. Yue, Y.L.; Sun, S.L.; Zuo, X. Discrete-time robust H<sub>∞</sub>/H<sub>2</sub> optimal guaranteed performance control for riser recoil. *Ocean. Eng.* **2024**, *304*, 117699. [[CrossRef](#)]
40. Dong, F.; Yuan, B.; Zhao, X.; Ding, Z.; Chen, S. Adaptive robust constraint-following control for morphing quadrotor UAV with uncertainty: A segmented modeling approach. *J. Frankl. Inst.* **2024**, *361*, 106678. [[CrossRef](#)]

41. Slotine, J.J.; Li, W. *Applied Nonlinear Control*; Prentice Hall: Englewood Cliffs, NJ, USA, 1991; Volume 199.
42. Wang, L.X. Stable adaptive fuzzy control of nonlinear systems. *IEEE Trans. Fuzzy Syst.* **1993**, *1*, 146–155. [[CrossRef](#)]
43. Majid, M.Z. Robust adaptive backstepping control of uncertain fractional-order nonlinear systems with input time delay. *Math. Comput. Simul.* **2022**, *196*, 251–272.
44. Ioannou, P.; Sun, J. *Robust Adaptive Control*; Prentice Hall, Inc.: Englewood Cliffs, NJ, USA, 1996.

**Disclaimer/Publisher’s Note:** The statements, opinions and data contained in all publications are solely those of the individual author(s) and contributor(s) and not of MDPI and/or the editor(s). MDPI and/or the editor(s) disclaim responsibility for any injury to people or property resulting from any ideas, methods, instructions or products referred to in the content.